
CONTROL-THEORETIC DRIVER MODEL DIFFERENTIATION BY LINEAR AND
NONLINEAR INPUT CUE COMPUTATION

L. LEUFKENS - 4090462

SUPERVISORS:

- 1) DR. IR. DAVID A. ABBINK
- 2) IR. SARAH BARENDSWAARD

Master of Science Thesis



DEPARTMENT OF BIOMECHANICAL ENGINEERING
FACULTY OF MECHANICAL, MARITIME AND MATERIALS
ENGINEERING

Contents

| | |
|--|-----------|
| Journal Article | 1 |
| Appendices | 10 |
| A Literature study | 11 |
| B Inherent identifiability of the nonlinear model | 41 |
| C Inherent identifiability of the linear model | 63 |
| D Single parameter analysis | 84 |

Control-theoretic Driver model differentiation by linear and nonlinear input cue computation

L. Leufkens¹ D.A. Abbink, S. Barendswaard

Mechanical, Maritime and Materials Engineering (3mE), Delft University of Technology, Mekelpark 5, Delft
e-mail: l.e.leufkens@student.tudelft.nl

September 13, 2018

ABSTRACT

Context. To investigate the effectiveness of nonlinear calculation of the near and far angle for driver modelling in curve negotiation, simulated data is analyzed based of Mars (7) driver model and the nonlinear realization of Mars model given in Scholtens (8).

Aims. It is shown that due to the dynamic calculation of the near and far angle, the simulated driver is less sensitive to change of the K_p or K_c parameter value during a drive. Static calculation of the near and far angle showed a wider range of drivers that can be identified before the start of the drive, but is less adaptable to change during the drive.

Methods. The range for the two parameters K_c and K_p was determined by setting two boundaries, whilst keeping the other parameters constant: the lateral position is bound to an absolute value of 1.8 meter and the steering wheel reversal rate to a maximum of 6. A ten by ten resolution range is subsequently established to form the basis for the simulations. The simulated results from the nonlinear and linear model are assessed on three criteria: realism, identifiability and descriptiveness. The three criteria show the realistic fit of the simulated data in comparison to real driver data (9).

Results. Static calculation of the near and far angle can capture a broader set of human drivers front end if the parameter set of the driver is know front end. A dynamic calculation is more adaptable to an unknown driver set and is therefor in a smaller need of knowing the driver before the drive starts.

Key words. driver modelling – human-machine interaction – curve cutting

1. Introduction

The interaction between humans and machines has seen a steady increase of research since the late 1960's and more profound in the past decade (1). This interaction can lend a crucial helping hand in task execution, navigation and inter robot and human communication. Car driving is a field in which a dynamic interaction between human and machine can improve overall safety of both the human driver and its direct surroundings.

Since the start of driver modeling, different angles of approach have been investigated to model the human behavior. There exist driver models and haptic interfaces based on hybrid metrics for adjustment of the haptic feedback (2), on direct measurable input (3)(4)(5) and on distraction parameters (6) which do not always have the steering wheel angle or position as a model output. Models which take a more microscopic approach would concern themselves with specific parts of a driver's journey, as car following or curve driving.

Automated driving is becoming an increasing part of daily life. Cars with parking control and force feedback on the steering wheel on the highway are Incorporated in an increasing amount of cars. Within this field of research, we aim to develop automatic systems that are able to help the driver as good as possible in its personal driving style. The personal driving style in curve driving should not be compromised by the automation and enable safe driving in every personal way. How to best be able to include cues from the automation, has not been concluded in earlier research. One of the open questions is with what parameters the human can be described in the automation,

and what values these parameters should be able to take. In this research a deep-dive will be made into two of these parameters, to see their effect on the driving style.

The goal of this study is to compare two realization of the Mars(7) driver model, based on the difference between the linear and nonlinear calculation of the near (θ_{near}) and far angle (θ_{far}). An adaptation of the Mars(7) driver model will be assessed as the linear model, and an adaptation of the realization Scholtens(8) made on the Mars(7) driver model will be assessed as the non-linear model. The comparison will be drawn by researching a parameter span of the two most sensitive parameters used in both models. A single parameter analysis, on the steering wheel angle and lateral position, concluded that the parameter set of [K_c K_p] had the highest change impact on the model. Therefor it is a key combination to adapting a driver model to uniquely being able to describe a human driver. K_c is the compensation gain acting upon the far angle (θ_{near}), and K_p the anticipation gain acting upon the near angle (θ_{far}).

2. Model elaboration

2.1. Model Background

In 2011 a driver model was proposed by Mars(7) et al (figure 1), which was based on the driver using visual cues and the car's speed, location and heading to determine the curvature of the road ahead. The identification, the human driver executes to determine the curvature of the road ahead, has been shown to be based on near and far regions in the driver's visual field. Mars(7)

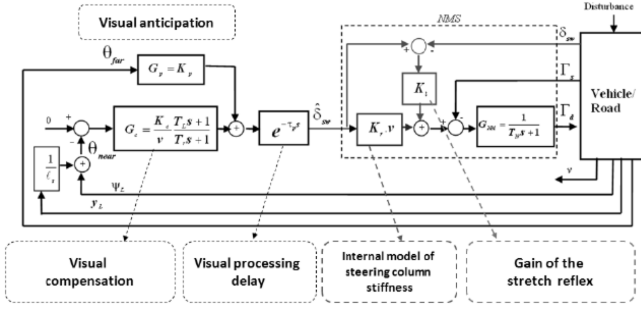


Fig. 1. Block diagram of the Mars Driver Model(7)

characterized these regions by identifying a near and a far point (figure 2). Where the near point (near angle θ_{near}) is used to stay

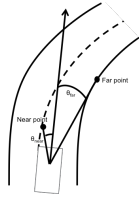


Fig. 2. Near and far point/angle

on the centre of the road, by looking a l_s distance ahead of the car. The far point (far angle θ_{far}), also used as the tangent point, is used to determine the future car trajectory based on the measured curvature of the road.

Mars hypothesized that human steering was a combined task of two components, a compensatory and an anticipatory part. The compensatory component uses the near angle θ_{near} to tune the driver to steer closer to the center of the road, by use of compensation equalization:

$$G_c = \frac{K_c T_{LS} + 1}{v T_{LS} + 1} \quad (1)$$

The anticipatory part uses the far angle θ_{far} and tunes the angle by use of the gain K_p . The anticipatory angle is added to the compensatory angle, before the combined result is slowed down by the time delay (τ_p) that is built in to simulate human behaviour. The proposed driver by Mars(7) derives a part of its methodology from McRuer(10). In 1977 McRuer proposed a driver model which used a feedback loop for the compensatory and the anticipatory part. The steering wheel angle would be described by:

$$\delta_{sw} = Y_y Y_\psi y_e - Y_\psi \psi + Y_\psi n \quad (2)$$

Where y_e is the lateral position error and ψ the vehicle heading. Y_y and Y_ψ are input dependent describing functions which McRuer to form a feedback loop for the compensatory part of the model and a feed-forward loop for the anticipatory part of the model.

Scholten(8) proposed a driver model in 2017, based on an the driver model proposed by van Paassen(12). Scholten hypothesized that a separated control structure would reduce conflicts between the driver model and the human compared to a coupled shared controller (figure 3). Scholten concluded that "providing the driver with guidance based on a combination

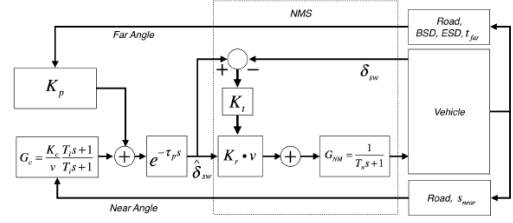


Fig. 3. Driver-model by Saleh(11), with a realization of Scholten(8)

of support and feedback torques is a promising approach to increase the acceptance" of the human to the machine. Future research should however continue on the focus of tuning the control parameters and further development of the driver model to ensure a better fit with individual human preferences.

The addition of nonlinear calculation of input cues to a driver model, results in a real time involvement in the calculation of the next car position to be reached. In the driver model proposed by Scholten(8), the dynamic calculation is included in the calculation of the near and far angle. Due to this nonlinear cue calculation, the model is more adaptable to a change in human driver parameter value change.

The driver model has 7 degrees of freedom (figure 4) The end-steering-distance (ESD), begin-steering-distance (BSD) and t_{far} influence the moment a driver starts anticipating a curve and when it stops anticipating on the curve it is in. The begin steering distance determines what distance the car has to be form the beginning of the curve to switch the target form the center of the road to the inside of the curve. t_{far} then determines the distance ahead of the car where the target point is placed. The end steering distance determines when the target point switches back to the centre of the road.

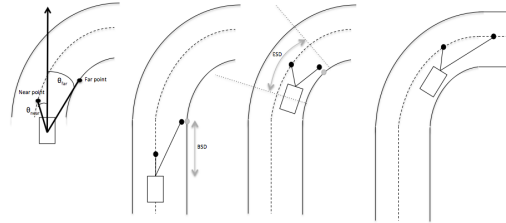


Fig. 4. End steering distance and begin steering distance with respect to the position of the car with respect to the curve

2.2. Neuromuscular Loop

Originally, in both the linear and the nonlinear model, a feedback loop (5) was included that proposes a way to include neuromuscular signals by applying two different gains of the steering wheel angle. First off, the neuromuscular system executes a steering torque on the steering wheel, which can be calculated with a gain (K_r) to the desired angle δ_{sw} . Secondly, a gain (K_v) was added affecting the vehicle speed. This neuromuscular loop has been excluded from the analysis because the vehicle dynamics used in this research take angles as input instead of torque. The neuromuscular loop takes place in between the time delay and the vehicle dynamics block.

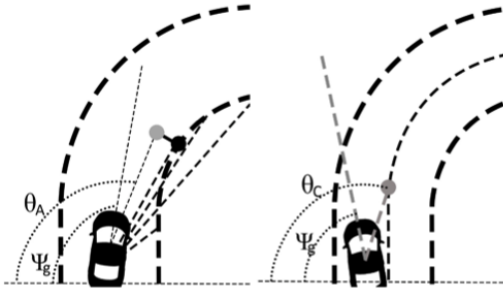


Fig. 9. Angle Calculation Nonlinear Model

In the θ_{near} calculation, s_{lat} is the lateral position, l_p the look-ahead distance and H_{error} the heading error angle. In every simulation step these two angles are calculated anew, based on the current car position.

As can be seen in the calculation of these two angles the two models differ in the linear versus nonlinear calculation of the angles. The more complex nonlinear calculation of the angles could be hypothesized to be more realistic and would therefore result in a better fit with real human test data.

The driving behaviour in a curve can be described in the difference between curve cutting and over steering behaviour (figure ??). Human driver generally tend to show different behaviour

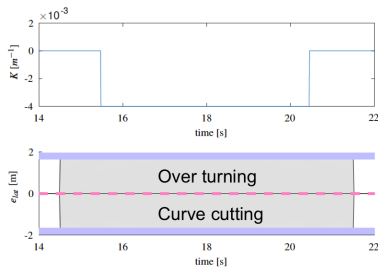


Fig. 10. Curve Behaviour Visualization (9)

in right opposite to left curves, which is described more in depth in the section ‘Results’.

3. Assessment procedure

3.1. Input determination

Both models are executed with a same list of parameters, used to describe human driving behaviour in the simulated data:

| | |
|----------|-----------------------------|
| K_p | Anticipation gain |
| K_c | Compensation gain |
| τ_p | Time delay |
| T_l | Lag-time constant |
| T_L | Lead-time constant |
| T_N | Neuromuscular time constant |

These parameters have been individually assessed on their effect on the simulated output of the models. In this assessment, the sensitivity of the individual parameter was first researched and afterwards, a combined sensitivity when paired with another

parameter. This individual parameter assessment showed that by ranging the values for the K_c and K_p parameters simultaneously, the clearest differentiation could be shown between a linear and nonlinear model. The main reason behind this is the fact that K_c as the compensation gain effects the θ_{far} angle and K_p as the anticipation gain effects the θ_{near} angle. The other parameters are kept to the nominal values determined by Saleh (11).

| | | |
|----------|-----------------------------|------|
| τ_p | Time delay [sec] | 0.03 |
| T_l | Lag-time constant | 1 |
| T_L | Lead-time constant | 3 |
| T_N | Neuromuscular time constant | 0.1 |

In order to make a clear assessment on the best and most realistic fit of a model with human driving, the simulated data has been assessed on three different criteria, following the method proposed by Barendswaard (9):

- **Realism**

The parameter span resulting in realistic driver outputs

- **Identifiability**

The uniqueness of the mapping between a driver type and a parameter combination (inherent and experimental)

- **Descriptiveness**

The extent of the model to capture different types of driver behaviour

On basis of the results on these three analysis criteria, conclusions can be drawn on how well the model fits real driver data. After the analysis of the real driver data fitting, the results can be compared with the same analysis on the other model, resulting in a conclusion of which driver model method fits human driving behaviour best.

The in- and outputs for this assessment method are depicted in figure 11(9). In the comparison of the two driver models, the

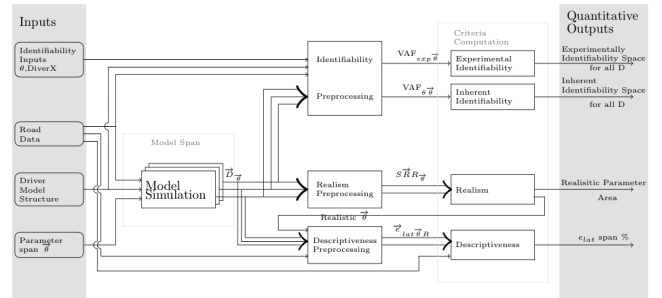


Fig. 11. Flow diagram of the Assessment Method (9)

main input is the driver model structure, the third input. The other inputs are kept constant over the two analyses. The first input, identifiability inputs, entails the parameter set Θ and Driver X real driver data derived from the human experiment executed by Scholtens(8). The road data used comes from the same human experiment by Scholtens and the same parameter span Θ is used for the model simulation.

The parameter span Θ has been derived by setting boundary settings, set as realistic. The first boundary setting is set on the lateral position of the car on the road, as a maximum deviation from the center line of it’s lane to 1.8 meter. The second boundary setting is set to a maximum and minimum steering wheel reversal rate. The steering wheel reversal rate is the amount of times, in a set period of time, that the steering wheel changes its angle by more than 2 degrees. Based on the averaged runs of the human driver set (Driver X) the realistic maximum, over a road with 1

left and 1 right curve, is 22 reversals. Since the driver models don't include a noise signal that can reciprocate human jitters, a maximum SRR of 22 results in unrealistic steering wheel angles, still staying within the lateral position boundaries. Due to the absence of noise in the model, Barendswaard (9) proposed to set the maximum SRR to 5 for 2 consecutive curves. The non-linear model has such a low descriptiveness (figure 12) when it is bound by an SRR maximum of 5, that the conclusions from an analysis would be difficult to sustain. It is not possible for a human being to reach a SRR of 2.5 in 1 curve. Therefore the maximum SRR for 1 curve is rounded, resulting in a maximum SRR of 3 per curve. Concluding the SRR has been extended to a value of 6, with a maximum SRR of 3 per curve. With this maximum bound, the descriptiveness of both the linear and nonlinear model lie above 30%, with which a proper analysis can be run.

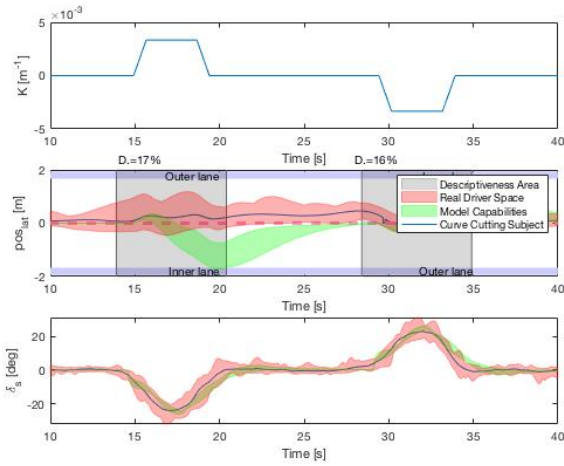


Fig. 12. Non linear model descriptiveness with a maximum bound to the steering wheel reversal rate of 5

Based on these boundary settings, the parameter span was computed to be:

$$\begin{aligned} K_p & [0 - 27] \\ K_c & [0 - 6.3] \end{aligned}$$

The parameter span is set to include the area in which both the lateral position bound and steering wheel reversal rate bound are met (figures 13 and 14). Based on the inputs, a quantitative output is computed which will be used to compare the two models as a model grade.

3.2. Identifiability

The inherent identifiability evaluates the extent to which the time series of a model can uniquely be identified by its own time series again. In contrast to that, the experimental identifiability evaluates the extent to which the simulated time series can uniquely identify a real human driver time series. The identifiability is measured by the Variance Accounted For (VAF). The VAF is a percentage, showing how well two signals coincide with each other. The higher the VAF value is, the better two set of signals match. The VAF is calculated as followed:

$$VAF = \left(1 - \frac{\sum_{k=1}^N |u_{driver}[k] - u_{mod}[k]|^2}{\sum_{k=1}^N u^2_{driver}[k]}\right) * 100\% \quad (20)$$

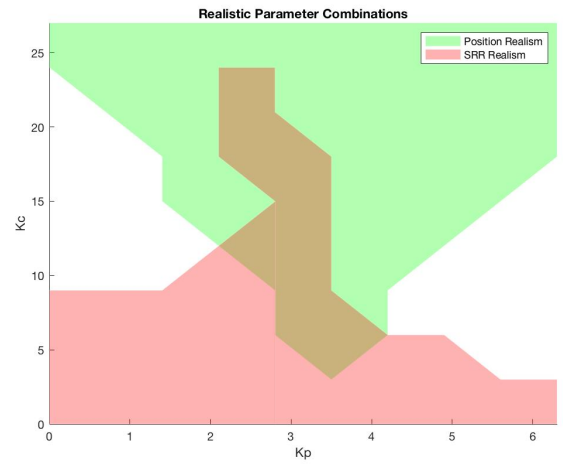


Fig. 13. Boundary Setting Linear model

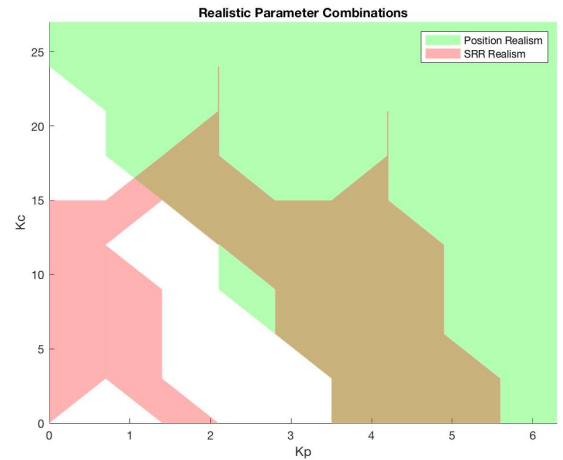


Fig. 14. Boundary Setting Nonlinear model

3.3. Realism

The second criterion, the realism, evaluates the chosen parameter span based on the steering wheel reversal rate. The steering wheel reversal rate (SRR) is defined as the number of times that when the steering wheel angle is changed, the difference is bigger than 2 degrees.

3.4. Descriptiveness

The third criterion, the descriptiveness, evaluates the extent to which the driver model is able to identify different types of driver behaviour. The descriptiveness is a percentage describing the total area the simulated data covers in a curve. The total area is described as the area from the start of the curve to the end of the curve with an extra second before and after the curve, with a maximum and minimum bound set as the upper and lower

limit, 1.8 meter and -1.8 meter respectively. For every time step the maximum and minimal position value is used as the outer bounds of the simulated driver area. The descriptiveness area is calculated as the area the simulated area covers the total area.

4. Results

4.1. Descriptiveness

Figures 15 and 16 shows the descriptiveness criterium of the non-linear and linear model respectively. The two graphs consist

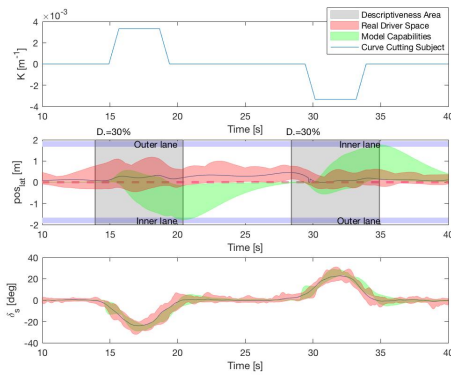


Fig. 15. Descriptiveness of the linear model

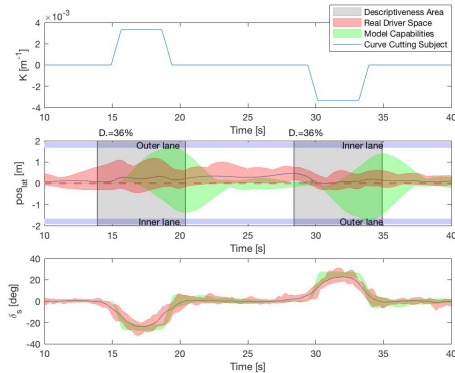


Fig. 16. Descriptiveness of the non-linear model

of three subplots. The top subplot shows the curvature profile of the 2 curves. The first bend is a right curve and the second bend a left curve. The middle subplot shows the road profile from a top view with the road limits on the top and the bottom in gray. The pink area shows the area of the road that is covered by the human drivers from the experiment. The green area shows the area of the road that is covered by the simulated data from the driver models. The light gray area shows the entire area that can be described in the curve. The descriptiveness percentage is described as the curve area covered by the simulated model area. A significant difference is seen in the curve driving behaviour that can be described with the two different models. The linear model shows the ability to describe both curve-cutting as overturning behaviour (figure 10), Whereas the non-linear model that even though it can describe a larger over turning behaviour area, it can hardly describe any curve cutting behaviour.

4.2. Identifiability

The identifiability criterium is displayed in the figures 17, 18, 19 and 20. The figures show the amount of overlap in data when comparing two sets of data with each other, from which we can conclude how unique a set of data is.

Figures 17 and 19 show the inherent identifiability, where a specific array of simulated data (in the figure chosen with the optimal experimental identifiability, linear $K_p = 3.5$ $K_c = 3$ and nonlinear $K_p = 3.5$ $K_c = 21$) is compared to the entire matrix of simulated data with ranging K_c and K_p . A significant difference

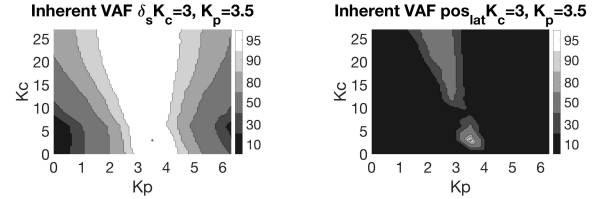


Fig. 17. Linear Inherent Identifiability

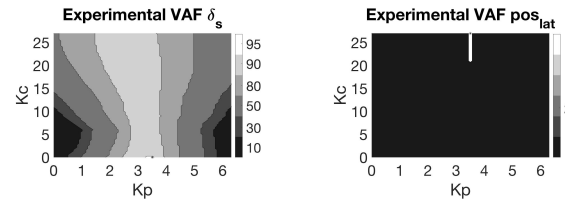


Fig. 18. Linear Experimental Identifiability

can be seen in the VAF of the steering wheel between the two models. The non-linear model shows to be less sensitive range to a change in a parameter than the linear model is. This can be described by the dynamic calculation of the near and far angles in the non-linear model, making it more adaptable to sudden change.

Figures 18 and 20 show the experimental identifiability. The driver data of the 16 human participants of the experiment have been averaged to compare with the matrix of simulated driver data. The experimental analysis of the steering wheel show the

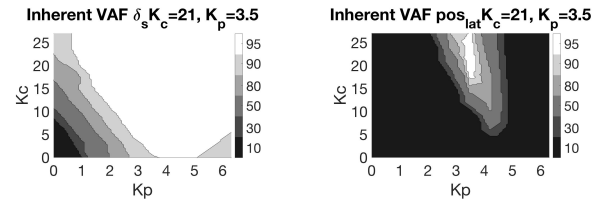


Fig. 19. Non-Linear Inherent Identifiability

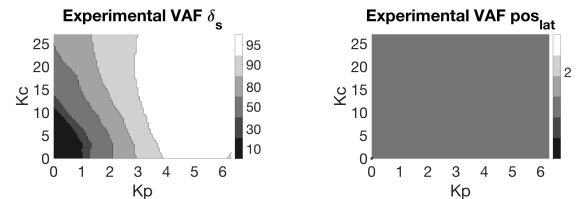


Fig. 20. Non-linear Experimental Identifiability

same difference in identifiability as the inherent analysis, where

the non-linear model is better adaptable to a change in K_C or K_p value.

The experimental identifiability of the lateral position show extremely low values when compared to the inherent identifiability plots. This is explained by the fact that even though the steering wheel angles may match up, the lateral position data does not when we look at left curves specifically. Where humans have the tendency to overturn curves when steering to the right, they tend to cut the curve when steering to the left. The experiment was executed in a simulator in the Netherlands. In the Netherlands humans drive on the right side of the road, which could explain the curve cutting behaviour in right curves. This could hypothetically result in a better visual what is coming up in a curve when it is a left curve as opposed to a right curve, maybe explaining why humans tend to curve cut left curves and over turn right curves. As a test of this hypothesis a simulation was

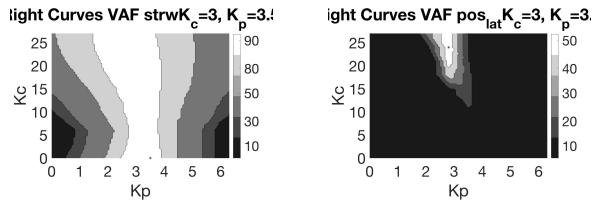


Fig. 21. Linear experimental identifiability, averaged over the 5 right curves in the road profile, $K_C = 3$ and $K_p = 3.5$

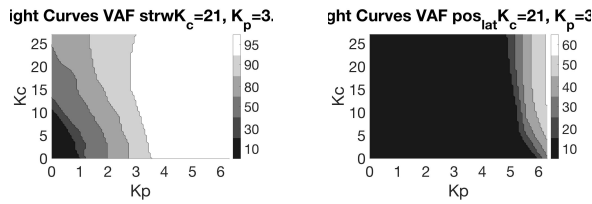


Fig. 22. Non-linear experimental identifiability, averaged over the 5 right curves in the road profile, $K_C = 21$ and $K_p = 3.5$

executed where the data was filtered to only use the right curve data. The resulting experimental VAF is shown in figures 21 and 22. In these plots a significant increase is seen in the mapping of the experimental data. The maximal VAF values have gone up from 0% to around 50 %. This can be explained by the constant values for the parameters ESD, BSD and t_{far} . These values apparently are set to result in a better simulation of right curves as opposed to left curves.

4.3. Realism

Figures 23 and 24 show the realism criterium of the linear and non-linear model respectively. The plots are divided up in three subplots. The top subplot shows the heatmap of the steering wheel reversal rate (SRR), depicting the amount of times a steering wheel change in the first two curves was larger than 2%. This plot can give an easy visual representation of how the steering reversal rate changes, even when it is outside of the realism bounds as set in figures 13 and 14. The plot doesn't look the same as figures 13 and 14, because the boundaries in figure 23 and 24 are not set to show the outer bounds of the realistic bound. The plot shows to what length the steering wheel reversal rate would become unstable and big when the setting does not lie in the realistic bound. The steering wheel stays relatively stable however,

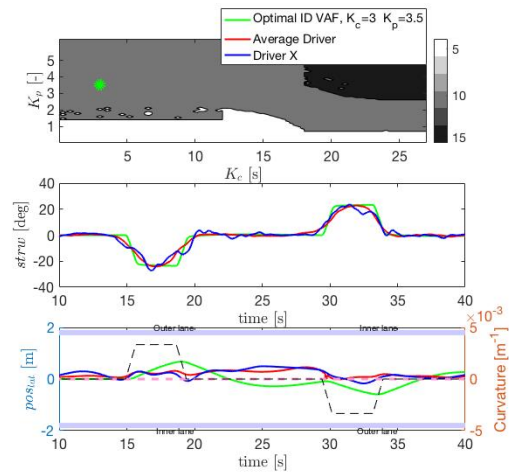


Fig. 23. Linear Realism

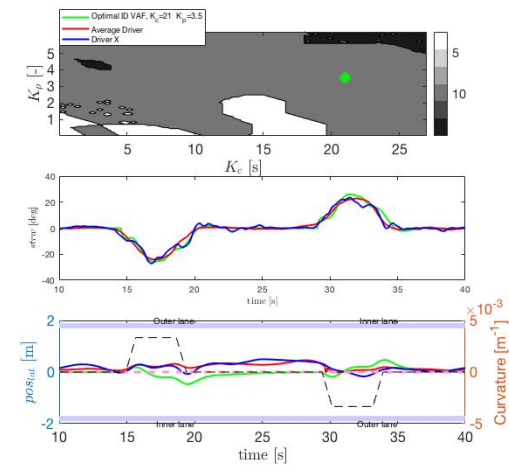


Fig. 24. Non-linear Realism

even outside of the realistic bound, with a maximum value of 15 reversals for the maximum values of K_C and K_p .

The middle plot and the bottom plot show the steering wheel angle and lateral position respectively. The bottom two subplots show three different lines. The optimal ID VAF is the combination set of the K_C and K_p value which resulted in the highest VAF for the experimental identifiability of the steering wheel angle, in the realistic area as seen in figures 13 and 14. The average driver line is the average driving style, averaged over the 16 participants of the human experiment. The Driver X line, depicts the single driver, from those original 16, who's driving style matched the average driver style best when looking at the lateral position on the road.

As was also seen in the descriptiveness criterium graph, the optimal ID VAF, is a curve-cutting line for the linear model and an over turning line for the non-linear model.

5. Discussion

The original expectation was that the non-linear model would be better in describing a wider range of driver behaviour. This expectation was based on the dynamic calculation of the near and far angle, as opposed to the static calculation in the linear model.

The results tell a different story however. Even though the non-linear model is shown to be less susceptible to change, it doesn't describe curve-cutting behaviour well. The linear model shows to be more sensitive to parameter change but on the other hand is able to describe both curve-cutting and over-turning behaviour. The main cause for this lack of descriptiveness by the non-linear model is the fact that, even though the model is a 7 degree of freedom model, only 4 degrees of freedom are used. The end-steering-distance (ESD), begin-steering-distance (BSD) and t_{far} are kept constant throughout the simulations. Therefore the following recommendations are summarized to enable future research to capture a complete analysis:

- Addition of variability in the 3 extra degrees of freedom non-linear model (ESD, BSD, t_{far})
- Addition of human like noise to be able to make the steering more realistic
- Inclusion of the Kr, Kt loop to include a hypothesized part of the Neuromuscular System
- The descriptiveness criterium could be elaborated on by adding a percentage for the area of experimental data covered by the simulated data. Realistically speaking, a human would never be able to cover the whole 100% of the depicted descriptiveness area, which could make the descriptiveness percentage biased. It could be more interesting to look at the percentage of the experimental data covered by the simulated data.

6. Conclusion

The method of comparison between the two models has been chosen as the set example by Barendswaard(9). This comparison can show a complete image of the capabilities of the two models, enabling an easy comparison.

From the results we can conclude the following:

- The linear model is more sensitive to change of the value of K_p or K_c than the non-linear model.
- The linear model shows a higher, but more importantly wider, descriptiveness area than the non-linear model.
- The non-linear model performs well in describing over-turning behavior, but bad in describing curve-cutting behavior for the limited parameters we looked into, with fixing the ESD, BSD and t_{far} parameter values.

References

- [1] J. Hoc, *From human – machine interaction to human – machine cooperation*, in Ergonomics, 2000, vol. 43, no.7, 833-843, 2000.
- [2] H. Okuda, N. Ikami, T. Suzuki, Y. Tazaki, K. Takeda, *Modeling and analysis of driving behavior based on a probability-weighted ARX model*, in IEEE TRANSACTIONS ON INTELLIGENT TRANSPORTATION SYSTEMS, VOL. 14, NO. 1, MARCH 2013, 2012.
- [3] C.J. Nash, D. J. Cole, Robert, S. Bigler, *A review of human sensory dynamics for applications to models of driver steering and speed control*, in Biological Cybernetics June 2016, Volume 110, Issue 2–3, pp 91–116, 2016.
- [4] W.H. Levison, J.L. Campbell, K. Kludt, A.C. Bittner, *Development of a drive vehicle module for the interactive highway safety design model*, in FHWA-HRT-08-019, Federal Highway Administration, 2007.
- [5] C. Sentouh, P. Chevrel, F. Mars and F. Claveau, *A sensorimotor driver model for steering control*, in Proceedings of the 2009 IEEE International Conference on Systems, Man, and Cybernetics, 2009.
- [6] Y. Dong, Z. Hu, K. Uchimura, N. Murayama, *Driver Inattention Monitoring System for Intelligent Vehicles: A Review*, in IEEE Transactions on Intelligent Transportation Systems, Volume: 12, Issue: 2, June 2011, 2001.
- [7] F. Mars, L. Saleh, P. Chevrel, F. Claveau, J. Lafay *Modeling the Visual and Motor Control of Steering with an Eye to Shared-Control Automation*, in Proceedings of the Human Factors and Ergonomics Society, 2011.

- [8] W. Scholtens, S. Barendswaard, D. Abbink *Reducing conflicts in Haptic Shared Control during curve negotiation*, 2018.
- [9] S. Barendswaard, D. Pool, D. Abbink, *A Method to Assess Individualized Driver Models: Descriptiveness, Identifiability and Realism*, in 2017 Driving Simulation Conference, Stuttgart Germany, 2017.
- [10] T. McRuer, R. Wade Allen, D.H. Weir, R.H. Klein, *New results in driver steering control models*, in HUMAN FACTORS, 1977, 19(4),381-397, 1977.
- [11] L. Saleh, P. Chevrel, F. Claveau, J.F. Lafay, F. Mars, *Shared steering control between a driver and an automation: Stability in the presence of driver behavior uncertainty*, in IEEE Transactions on Intelligent Transportation Systems, Volume: 14, Issue: 2, June 2013, 2013.
- [12] R. van Paassen, R. Boink, D. A. Abbink, M. Mulder, and M. Mulder, *Four design choices for haptic shared control*, in Advances in Aviation Psychology, Volume 2 – Advances in Aviation Psychology (pp. 237 - 254), 2017.

Appendices

Appendix A

Literature study

Literature Study
Master Thesis

David Abbink
Sarah Barendswaard
Lotte Leufkens
+31 6 27 07 34 34
lotteleufkens@gmail.com

May 27, 2017

Contents

| | | |
|----------|---|-----------|
| 1 | Introduction | 3 |
| 2 | Experimental Evidence for Inter-Driver Variability | 4 |
| 2.1 | Inter human variability based on vehicle based parameters | 6 |
| 2.1.1 | Position | 6 |
| 2.1.2 | Velocity & Acceleration | 7 |
| 2.2 | Inter human variability based on gaze based parameters | 8 |
| 2.3 | Near & Far point | 9 |
| 2.4 | Tangent point | 10 |
| 2.5 | Occlusion point | 11 |
| 2.6 | Future path | 11 |
| 2.7 | Splay angle | 12 |
| 2.8 | Conclusion | 12 |
| 3 | Driver models | 14 |
| 3.1 | Sensorimotor model | 15 |
| 3.2 | Adapted two-point | 16 |
| 3.3 | Boink | 16 |
| 3.4 | Separating Haptic Guidance and Support Signals | 18 |
| 4 | Discussion & Conclusion | 19 |
| 4.1 | Discussion | 19 |
| 4.2 | Conclusion | 20 |
| | Appendices | 21 |
| A | Driver model comparison | 22 |

Chapter 1

Introduction

The interaction between humans and machines has seen a steady increase of research since the late 1960's and more profound in the past decade [1]. This interaction can lend a crucial helping hand in task execution, navigation and inter robot and human communication. Car driving is a field in which a dynamic interaction between human and machine can improve overall safety of both the human driver and its direct surroundings.

This literature survey will serve as a basis for further research on the optimal cooperation between human and machine interaction when it comes to car driving. The main research question that will be answered is:

‘What individual differences occur in steering behavior during curve negotiation and what model best describes these differences?’

Which, for the purpose of simplification, is subdivided as follows:

- What individual differences in steering behavior occur during curve negotiation
- What realistic and tested driver models exist

The review in human variability is scoped to previously tested and applicable metrics. The metrics used in the variability review are used to scope the driver model review in chapter 3. These metrics are both conscious and unconscious behaviors executed by the human during driving, divided in the categories ‘vehicle based parameters’ also called Newtonian parameters and ‘gaze based parameters’.

For the purpose of the comparison between human driver models an absolute comparison has been written which can serve as a tool to choose a model for further research (Appendix A). Depending on the topic of the further research a different model from the comparison could be chosen to fit best.

The most important metric throughout this paper is ‘variability’. The opportunities to explore inter human variability and how to in-cooperate variability in a driver model can play a crucial future role in development of human-machine cooperative car driving.

Chapter 2

Experimental Evidence for Inter-Driver Variability

Driving is, and has always been, a complex task with multiple components, in need of different human cues for safe execution. One needs their eyes to see the road, their ears to hear the nearby cars, and hands to translate all the different inputs into the right maneuvers with the car. One is also in need of knowledge of the traffic law, the route to take to get home or how to adapt speed with animals nearby.

In order to share the control of the vehicle movement with an automated system, the human must still be as able to perceive the vehicle's state as before, if not even better by the feedback the system can provide. It is therefore highly important that the form of communication between the human and automation is clear and precise to both sides. A mismatch in the communication between human and machine can cause overcompensation from both sides to fix the mismatch, causing the vehicle's trajectory to become uncontrollable.

Since the start of driver modeling, different angles of approach have been investigated to model the human behavior. There exist models based on hybrid metrics for adjustment of the haptic feedback [12], on direct measurable input [5][7][11] and on distraction parameters [19] which do not always have the steering wheel angle or position as a model output. Models which take a more microscopic approach would concern themselves with specific parts of a driver's journey, as car following or curve driving.

A multitude of processes exist in which a human executes conscious and unconsciously how to get from A to B safely. These task processes can be identified by three classes for driving[15]:

- Operational processes, *the actual manipulation of control inputs*
- Tactical processes, *awareness of ones surroundings to keep the situation safe by safe inter-action*

- Strategic processes, *high end computing for tasks as route planning*

It comes around all but too often that for certain task processes not just one of these classes is used and needed for safe execution. The complexity that research has been trying to solve for decades has been the question how to capture these ‘abstract’ classes in measurable individual human differences.

This chapter shows in which ways inter human variability could possibly be captured in direct data. Data would be necessary to tell the automation what the human is doing and how the automation should possibly adjust to that behavior. Therefor this chapter will focus on the operational processes of human driving.

For the further research on this literature report the following definition is used for the inter human variability:

"An individual difference is a physiologically measurable output of a human driving task influenced by the task processing of the human in control."

For the case of simplicity the possible variability cues have been divided in ‘vehicle’ and ‘gaze’ measures. The vehicle measures could be directly fed back to the automation, correlating with the outputs controlled by the automation. The gaze measures tell a story about the physical state of the human being which would need a translation level to transform human physical states into usable input for the automation. Examples of vehicle outputs could be distance from the center line, longitudinal velocity and the relative curvature between car trajectory and road. Gaze outputs of human behavior could be the visual points drivers use for path planning.

Studies conducted in the past do entail on the difference in driving performance[33], such as shown in figure 2, but not in driver variability. If these figures would also show the

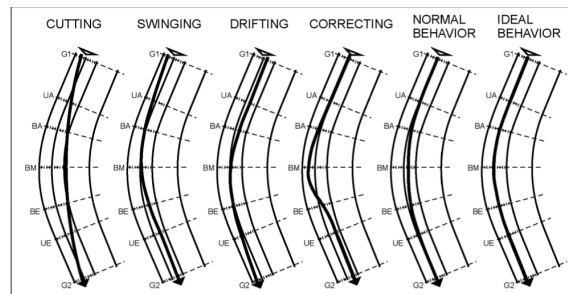


Figure 2.1: Sketch of different curve cutting

standard deviation and the differentiation from the mean, a measure of variability would be available. This figure shows that difference exists in the driving performance between humans using naturalistic data.

2.1 Inter human variability based on vehicle based parameters

As mentioned in the chapter introduction, driving processes can be divided into three processes, as proposed by Michon [25]: operational, tactical and strategic. A similar model of hierarchical division of the driver's tasks is Rasmussen's model of knowledge-based, rule-based, and skill-based behaviors. These definitions have great overlap, since the strategic behaviors happen at the knowledge-based level, tactical at the rule-based level and operational behaviors occur at the skill-based level. In this subsection the focus will lay on the operational processes which happen at skill-based level, which are processes that are highly automated in the human behavior due to much practice. In general drivers don't actively think about the actions taken to reach their desired outcome.

The outcome of these unconscious processes are the position, velocity and acceleration of the car on the road. Every human has a different and preferred position and velocity with respect to center lines, other cars and trees for example.

2.1.1 Position

The position of the car with respect to road markers is a distinctive manner of differentiating between driver preferences. These can be defined by the distance between car and for example center lines, trees, other cars, road edges and trucks. A multitude of studies have been executed on whether the adaptation to these metrics happens consciously or not, where for example the road width seems to yield a implicit perceptual human response [26]. Hess(1990) goes so far as to say that "The characteristics of a good driver/vehicle system can be succinctly described in control terminology as those which cause the output $y_v(t)$, to equal the input $y_r(t)$ over as broad a frequency as possible" [30], relating the lateral position error to the desired lateral position on the road 2.1.1. Using the same input as output parameter reduces the complexity of the system.

A second position based parameter is the heading angle as an input for the automation. Usually in combination with the lateral error, the desired and actual heading angle are compared a certain 'look-ahead' time in front of the car [30]. The heading angle is in general defined as the angle on the body axis of the car with respect to the defined neutral angle of your x-y axis system. The heading angle error is the degrees difference between the angle of the vehicle body axis and the angle of the center line of the road, usually chosen a distance in front of the car 2.1.1. This distance is in general defined as a certain time span from which the distance can be derived when the car's velocity is known. Equivalently a relative high look-ahead-time would result in a relative small heading angle error.

Figure 2 shows that there is a distinct difference between the way humans position themselves on the road, however not displaying the variability by measures such as the standard deviation. This figure is derived from a typology study done by Peter Spacek [33] to show the inter human variability in curve cutting.

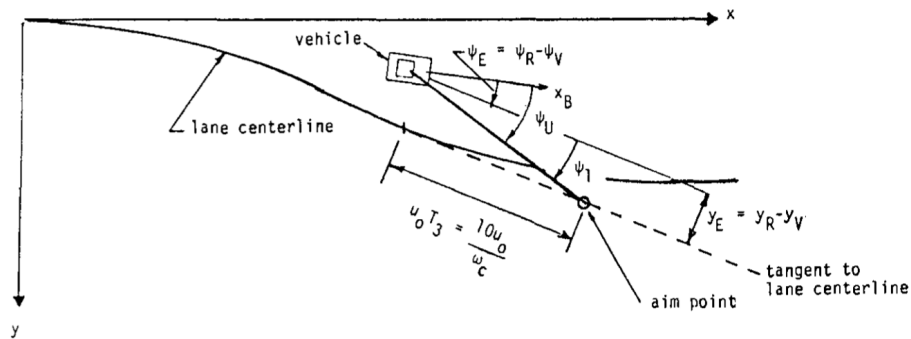


Figure 2.2: Visual representation of the lateral error (y_v) and the heading angle error (ψ)[30]

2.1.2 Velocity & Acceleration

Tracking these position markers over time results in velocities, and indicatively, the relative velocity between the car and its surroundings. This consists of the lateral and longitudinal velocity, the velocity in line with the heading angle and at a right angle with the heading respectively.

Especially in bends the tracking of the acceleration or deceleration can show inter human differences in lateral and longitudinal direction. Research studies and experimental studies

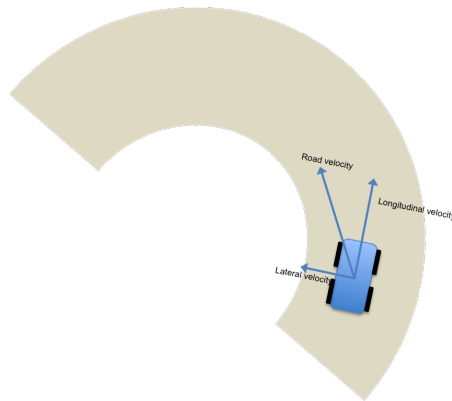


Figure 2.3: Visual representation of the lateral and longitudinal car velocity during curve driving

show that humans adapt the velocity and acceleration of the car so that maximum vehicle lateral acceleration is decreased at high speeds [27]. Reymond and Kemeny (2001) propose a model which would include an acceleration safety margin therefor in case unsuspected deviations of the trajectory occur [27]. They recorded the variability in accelerations during

the curves in their test track and used their model to adjust the speed of the car to have a safe vehicle lateral acceleration.

| | Dynamic Simulator | | | Static Simulator | | |
|--------------|-------------------------------|---------------------------------|-------------------------|-------------------------------|---------------------------------|-------------------------|
| | Γ' (m/s ²) | $\Delta C'$ (km ⁻¹) | e (m/s ²) | Γ' (m/s ²) | $\Delta C'$ (km ⁻¹) | e (m/s ²) |
| Participants | | | | | | |
| S1 | 7.92 | 5.99 | 0.93 ($r = .83$) | 8.46 | 4.10 | 1.11 ($r = .71$) |
| S2 | 6.52 | 3.31 | 0.83 ($r = .90$) | 7.78 | 2.90 | 0.95 ($r = .76$) |
| S3 | 8.77 | 6.21 | 0.77 ($r = .90$) | 8.26 | 3.42 | 1.10 ($r = .72$) |
| S4 | 8.60 | 7.19 | 0.82 ($r = .85$) | 9.21 | 4.17 | 1.21 ($r = .73$) |
| S5 | 8.52 | 4.90 | 0.64 ($r = .88$) | 7.40 | 4.34 | 0.88 ($r = .92$) |
| S6 | 7.73 | 4.49 | 0.98 ($r = .87$) | 9.11 | 2.91 | 1.20 ($r = .70$) |
| S7 | 7.90 | 6.62 | 0.75 ($r = .89$) | 8.18 | 4.93 | 1.42 ($r = .75$) |
| Mean | 7.99 (± 0.76) | 5.53 (± 1.36) | 0.82 ($\pm .11$) | 8.34 (± 0.66) | 3.82 (± 0.77) | 1.13 ($\pm .18$) |
| Controls | | | | | | |
| T1 | 8.30 | 6.81 | 0.81 ($r = .82$) | 8.88 | 7.40 | 1.00 ($r = .79$) |
| T3 | 8.13 | 9.64 | 1.13 ($r = .85$) | 9.20 | 10.59 | 0.79 ($r = .92$) |
| T5 | 8.32 | 8.34 | 0.76 ($r = .93$) | 7.59 | 7.75 | 0.77 ($r = .90$) |
| T6 | 7.55 | 8.63 | 0.88 ($r = .82$) | 7.99 | 5.97 | 0.99 ($r = .87$) |
| Mean | 8.07 (± 0.36) | 8.36 (± 1.17) | 0.90 ($\pm .16$) | 8.42 (± 0.75) | 7.93 (± 1.94) | 0.89 ($\pm .12$) |

Figure 2.4: Regression coefficients based on the accelerations driven in the simulators by the test participants [27]

2.2 Inter human variability based on gaze based parameters

When you disturb the vestibular human system it has been scientifically proven that driving performance and perception is affected (Clarke, Clarke & Schere 1996). Perturbations in the human physical state have an effect on the driving of the human. By this equivalent, tracking the human physical state is a source of information for the automation on how to assist the human during its driving.

Inter human variability can be tracked in measures which are not a direct car state. Tracking the physical state of the human being is however more complex than linking it to a direct car state. It will need an extra level of translation to be useful as input for the automation.

One of the most crucial components of the human in control is his eyesight whilst driving. With it he can capture his surroundings, the road, nearby cars and humans. It should therefore be no surprise that most of the research found focuses on the focus points of human eyesight on straight roads and in curves. The visual focus has become a big point of discussion from the very start where the driver's gaze was modeled by the position of one's head[16] up unto papers that argue with one another whether to work with a FP or a TP [3][2][17].

To understand the research parameters and global descriptions in this field of research this section will explain the meaning of the most common and useful variables. The visual paths the eyes follow can show what the driver will do in the following seconds, which with a translation, can be led into the automation as future trajectory.

2.3 Near & Far point

The two-point model designed by Salvucci and Gray [24] uses a ‘near’ and ‘far’ point to estimate the driver’s trajectory explicitly. To avoid having to calculate curvature in bends, the near and far point can be used on both straight road passages as curved ones. The near point is set at a short distance from the car such that it is near enough to monitor later position but far enough that the driver could easily see it from the driver’s seat. The far point is implemented to track lateral stability and maintain a predictive steering angle that compensates for the upcoming road profile. [24] It is hypothesized that these points

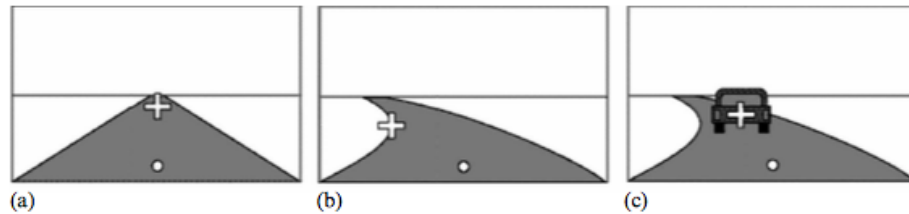


Figure 2.5: Near and far points for three scenarios: (a) straight road with vanishing point, (b) curved roadway with tangent point, and (c) presence of lead car [24]

are used by humans to calculate their trajectory. In studies such as the two-point model by Salvucci and Gray a calculated near and far point are used by the automation to adjust the automation’s corrective steering. The study looks at variability in the initial heading of the human instead variability in the landmark where humans put the near and far points 2.3. So it is a conceptual idea that these near and far landmarks are placed differently inter-human but not proven up to date.

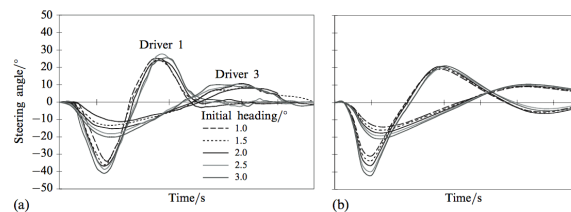


Figure 2.6: Difference in corrective steering force by the automation corresponding to a different initial orientation angle

2.4 Tangent point

The tangent point is a visual point in a driver's gaze on the inside curve of the bend. It is drawn on the point where the driver's gaze intersects with curvature of the inside bend. Several research papers [2][3] discuss the use of the tangent point by the driver and how this could be used for an improved driver model.

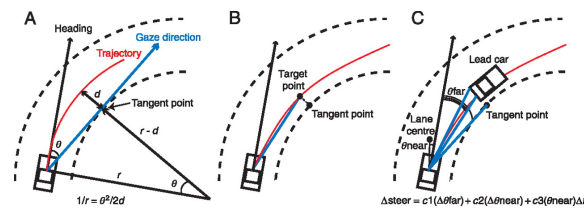


Figure 2.7: Tangent point on road [3]

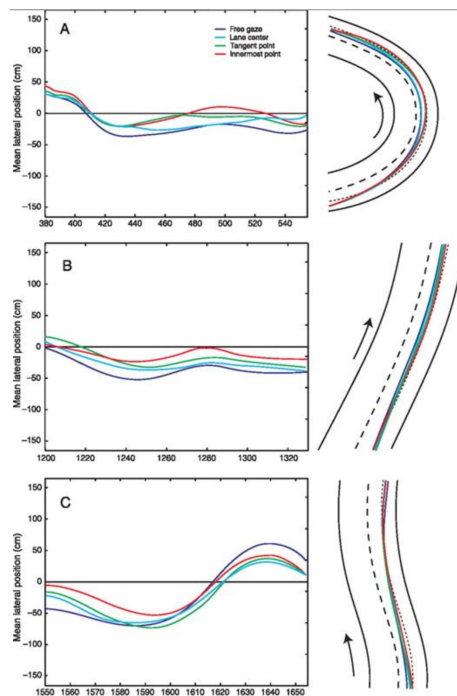


Figure 2.8: Lateral position of the car averaged across subjects in the study of Frank Mars [3]

Boer [35] uses the tangent point in his model such that the automation calculates an optimal trajectory based on target points on or nearby the tangent point. Boer however

did not take the variability of where humans put the tangent point into account, using 1 calculated tangent point. Mars [3] also uses a calculated tangent point to see how portrayed target gaze points affect the steering of drivers. The results of these studies did include variability in lateral position between human drivers, but did not show results on where the variability in gaze points go2.4.

2.5 Occlusion point

The occlusion point is the second visual point used for driver models. In Lehtonen et al. (2012) [22] it is defined as the point where the road disappears from view. Because the road has width, there is no such unique point. For example, there is one occlusion point on the future path as well as two occlusion points on the road edges and one on the road centerline, resulting in four occlusion points. [22]

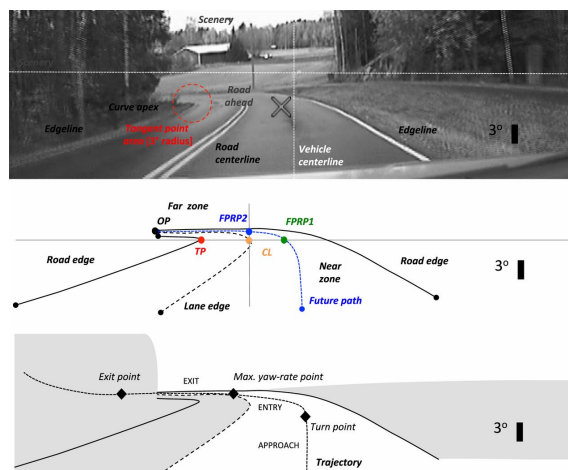


Figure 2.9: Visualization of TP, OP and FP[22]

2.6 Future path

The future path (FP) is visualized as the center-line trajectory of the car (2.9). On this path several points can be distinguished, ‘FP reference points’. These lie next to the tangent point on the same vertical visual line and are located on the future path. These future points have barely been used in studies thus far in field studies making the applicability complex and realism uncertain[22].

2.7 Splay angle

Calvert (1954) was the first to propose a different visual angle, named the splay angle. The splay angle is formed between the angle of the road marking relative to the vertical to control the lateral position on the road. It was first used in maintaining altitude in airplanes named the ‘optical splay’ by R. Warren (1982) and a derivative named ‘splay rate’. Loomis and Beall (1996) use this angle as an optical-flow rule to control their lateral position.

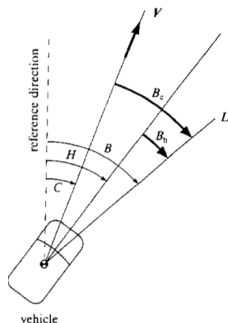


Figure 2.10: Shown here is a plan view of a vehicle traveling with velocity V , Course (C) is a measure of the angle between the vehicular velocity and a reference direction (such as North); whereas heading (H) is a measure of the angle between the longitudinal axis of the vehicle and a reference direction. Bearing (B) refers to the direction to a landmark (L) with respect to a reference direction (eg North). Two other pertinent concepts are course-relative bearing and heading-relative bearing. Course-relative bearing (B_c) is the bearing of a landmark relative to the course of the vehicle. and heading-relative bearing (B_h) is the bearing of a landmark relative to the heading of the vehicle.[34]

2.8 Conclusion

Studies have shown that inter human variability occurs in vehicle based parameters such as lateral position and accelerations [27] [30]. There would be a big field of further exploring these parameters and adaptation of the automation’s behavior on vehicle parameter variability. In the next chapter an exploration will be done with which existing driver models this would be possible.

The data coming from gaze tracking can lead to numerous interesting options for use in driver models. By deciding which of these visual cues to track and computing a fitting mathematical model these cues could be used to form a future trajectory. This future trajectory could in turn be used by the automation to adjust its heading angle and lateral

position as a direct output. At the same time they provide a source of information which corner points and visual way points are used by the human to compute the car's velocity and lateral acceleration [32].

Chapter 3

Driver models

In order to incorporate individual human variability in the automation loop, realistic operable driver models are necessary. For the scope of this literature study a broad search has been executed to touch upon the state of the art driver models and how these would or would not be useful for further research. Two of the biggest metrics in the decision making were, realism of the variability and complexity of the model.

The realism of the variability has been discussed in the previous chapter. Four of the best applicable models will be elaborated on in this chapter, where the scope has been narrowed to models which are based on Newtonian parameters (vehicle based). The gaze parameter models are not taken along in this chapter since their realism at this moment is lower than the vehicle based parameters. Studies have already been done that prove the variability in vehicle parameters [33], but none can be found that show the variability in between humans in landmarks such as the tangent point.

The entire analysis of existing driver models has been added in appendix A. Gaussian mixture models and model predictive control models have a certain level of complexity which made them impractical. These entail a large amount of gains in general which make it challenging to fully comprehend what is happening real-time. They do create a more realistic calculation of the action the driver automation should take.

A different approach with regards to driver modeling can be taken with respect to inputs, outputs and the working principle in between. Keeping an eye on the basis of research this literature review will need to provide, the scope of this review kept itself to realistic and tested driver models.

In order to provide a clear basis to compare the different models, the following sections will at least include the following aspects of the models: inputs, outputs, assumptions, limitations and a figure of the model structure. On the minimal basis of this information and the knowledge acquired by reading the papers further research could deduce with which model they could continue their specific part of research into human-automation cooperative driving.

3.1 Sensorimotor model

In 2009 a driver model was developed by Mars and Sentouh as part of the research program ‘Partage’ [11]. The model incorporates visual and kinesthetic perception, and compensatory and anticipatory processes.

As inputs the model uses the visual near and far point and the steering angel. The output is haptic force feedback on the steering wheel.

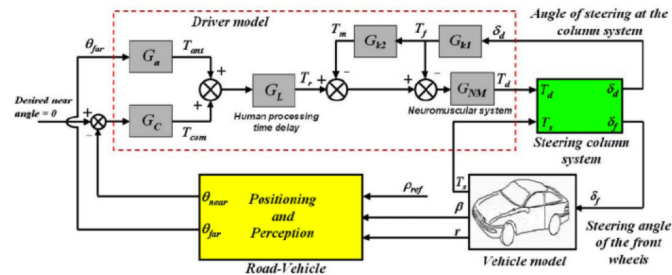


Figure 3.1: Two-point driver model [11]

By implementing the angle that is computed from the near and far point, the model doesn’t have to take preview time or the car velocity into account. The model does get more complex, due to the fact that the observation behavior needs to be modeled in this case, which would not be the case when using the prediction error.

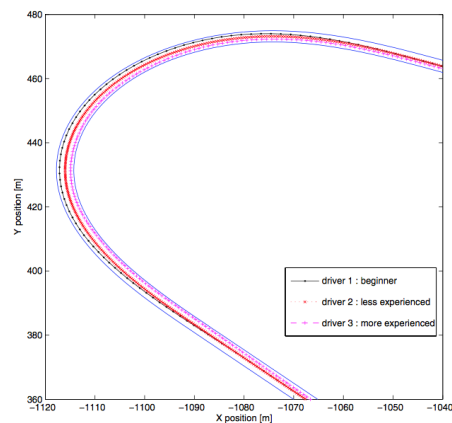


Figure 3.2: The response of the driver model for three different driving strategies [11]

The bigger drawback occurs when entering and leaving curves. The moment needs to be known when the driver starts looking at the tangent point and when this tangent

point disappears from view. To compensate for the disappearance of the tangent point, the model would keep the last calculated angle for the curvature tracking of the car until the curve ends.

The model looks at variability in the lateral position of the human driving 3.2 and has been tested in a simulator. The gaze points mentioned are calculated by the automation by which the automation adjusts its corrective steering.

3.2 Adapted two-point

The adapted two-point model3.3 is a feedback model, where "the anticipatory control is proportional to the actual curvature resulting in much more realistic driving behavior"[9]. This model is an elaboration on Sentouh's two-point model, where in this model a high gain in more severe corner cutting accordingly to the sharpness of a curve. This has advantages for both strong and short curves. In a bend the estimate of the curvature gets lower due to the fact that the vehicle will be closer to the inner lane boundary. Just as in the previous

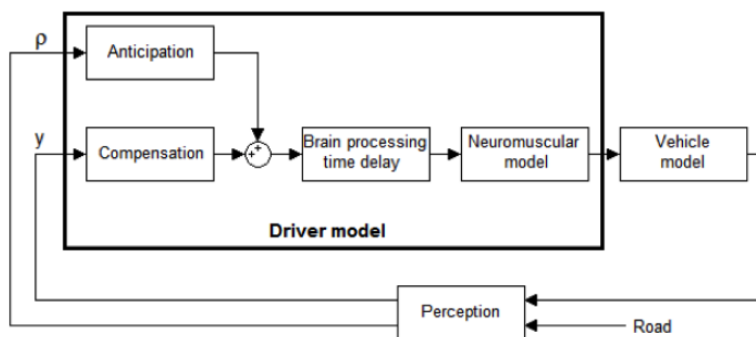


Figure 3.3: Adapted two-point driver model [9]

paragraph, the model takes variability in the lateral position on the road into account 3.2 and has been tested in a simulator.

3.3 Boink

In his paper [20] Boink discusses a driver model with adapted parameters of the look-ahead controller providing individualized guidance torques. The results of this study showed a positive influence on the match of desired steering wheel angles. The model described in his paper [20] was seemingly different from the model he actually tested with, which was a more simplified driver model given in figure 3.4. Boink's model makes use of the small-angle approximation in its feedback loop. When the angle is significantly small

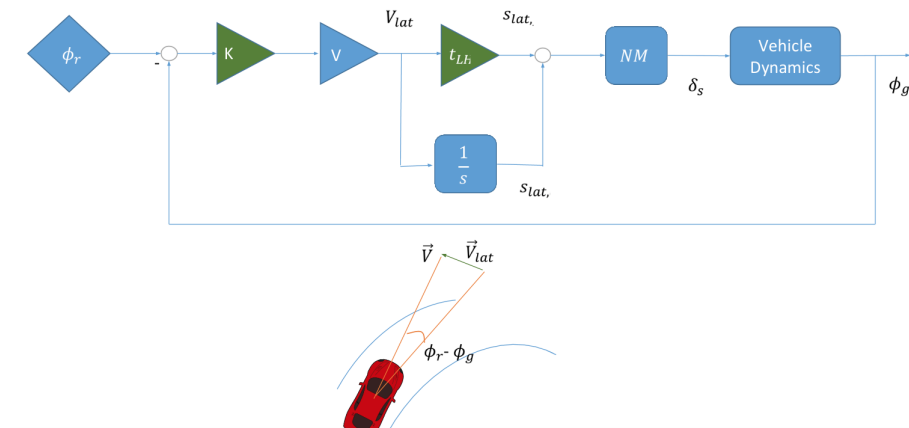


Figure 3.4: Boink's simplified driver model

enough the trigonometric function can be neglected and the angle can be fed back without computation.

The model makes quite a number of assumptions, making the model relatively unrealistic. Boink uses the variability in steering angle which is preferred by the current driver as input for the automation to compute its corrective steering force^{3.3}. By changing the look-ahead

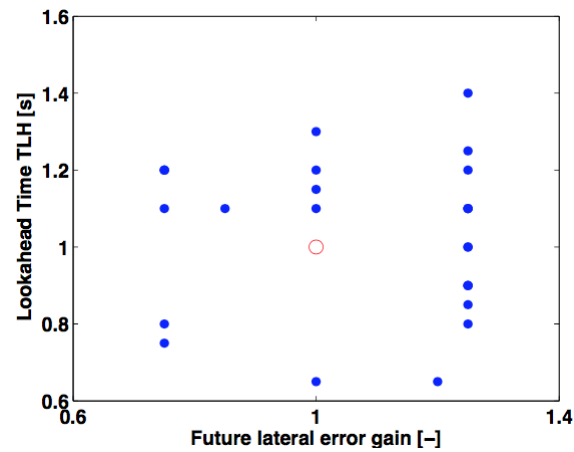


Figure 3.5: Individual fits of look-ahead time and lateral error gain used in Boink's experiment [20]

time, the green gain in figure 3.3 named t_{lh} changes value by which the addition circle next in the block scheme compares the current car position with one in the nearby future (depending on the look-ahead time). This model has been tested in a car simulator.

3.4 Separating Haptic Guidance and Support Signals

Professor Renee van Paassen has been working on a model using both feedback and feed-forward loops, using both the tangent point (or so target point) as the lateral deviation from a predefined reference trajectory [21]. The feedback loop is used for the reference

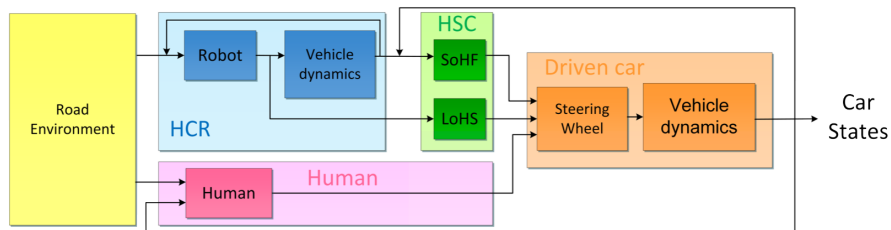


Figure 3.6: Haptic shared control architecture

trajectory driven by a so-called ‘ghost car’. The feed-forward loop is only used for the curvature in a bend. To simplify, the feed-forward loop tells you if you follow the correct curvature in the bend but this could be 6 meters from the center-line, the feedback loop doesn’t take the curvature into account but purely looks at the deviation from the center-line of your lane 3.6.

The biggest difference with Boink’s model is that Boink’s model looks at the road for the reference trajectory, whilst van Paassen’s model looks at the reference car for the feedback loop [23]. This reduces the overshoot when the feedback loop detects that you entered a curve or bend. This model has been tested in a simulation run with three different levels of

| Subject type | | K_{far} [-] | K_{near} [-] | t_{la} [s] |
|--------------|------------|----------------------|-----------------------|--------------|
| SS | Safe | 0.14 | -1.7 | 0.5 |
| SN | Neutral | 2.3 | -0.13 | 0.4 |
| SA | Aggressive | 2.5 | -0.1 | 0.7 |

Figure 3.7: Overview of the driving parameters for three different simulated drivers in an experimental set-up with the Van Paassen Model[23]

driving aggressiveness3.4. It tries to capture variability in lateral position, however, since it was only run in a computer simulation, this is purely conceptual. It entails the inputs lateral deviation and heading angle error in feedback and feed-forward loops to translate the human variability in a realistic human driver model and ghost driver to assist the human driver.

Chapter 4

Discussion & Conclusion

To conclude we look back at the research question initiating this literature research:

- What individual differences in steering behavior occur during curve negotiation
- What realistic and tested driver models exist

Based on the given scope, appendix A and the discussed realism this chapter will finalize a decision with a discussion and conclusion.

4.1 Discussion

The first part of the research question focused on the inter human variability. Based on literature this variability could be divided into two segments: vehicle and gaze parameters. Vehicle based parameters entailed direct car states such as lateral position, heading angle and velocity. Gaze based parameters entailed landmarks which theoretically humans use to orientate themselves in curves and plan their trajectory accordingly, such as tangent point, occlusion point and splay angle.

The gaze based metrics could provide exact and real-time data. For the scope of this literature study they would however prove to be unrealistic since people would be continuously driving with goggles, which is not an incorporated part in the driving culture yet. Vehicle based parameters would be better suiting metrics since the sensors necessary for position, velocity and acceleration control are already present.

To make a finalized decision, the research was extended in the review of driver models that worked with human variability. Deduced from a more extensive study four models have been reviewed in depth which worked with realistic Newtonian metrics. The vehicle based parameters have been discussed as best controllable, by which the sensorimotor model and adapted two-point model wouldn't be best for further research. The separation between haptic guidance and support signals entails a more complex and realistic model for the

human driving behavior than the model proposed by Boink. Boink's model operates on several assumptions solved by the models of Mars[3], Sentouh[11] and van Paassen[21].

4.2 Conclusion

Depending on the future research, several following roads can be taken. Based on the gaze parameters it could be very informative to conduct a research study to see if there is a significant variability in where different human place the landmarks such as the tangent and the extended tangent point. Since variability has already been proven to exist in vehicle based parameters, an elaboration could be made on a model working with vehicle based parameters to include inter human variability into the model.

If one would choose to investigate the existence of variability in gaze based parameters a good option would be to design a new driver model since none of the models researched for this literature study included the option to investigate inter human gaze variability. In the further exploration of using vehicle based parameters one of the four models from chapter three can be used to explore variability. Depending on the complexity the research would include, the model choice could land on Boink's model for simplicity or Mars', Sentouh's or Van Paassen's if the research would include a higher level of complexity.

Appendices

Appendix A

Driver model comparison

This appendix shows the models that have been investigated to see which models would be realistic options for further research in inter human variability. They are listed in chronological order, with the specific assumptions and concerns for every model listed next to it. The four models discussed in more depth in chapter three showed the most potential in realistic further research.

| Date | Driver Model | Inputs | Limitations & Boundaries | Feedback & Feedforward Multiple loops | Module structure |
|------|----------------------------------|--------|--|---|--|
| 1959 | McRuer [36] | 1 | Only valid in cross-over region, whilst most driving occurs at much lower frequencies. The model only applies to compensatory feedback and does not include preview. | Single feedback form | <p style="text-align: center;">(1)</p> |
| 1968 | Linear Prediction Model [9] | 1 | Driver modeled as simple gain without any brain processing or neuromuscular time delay. The fixed preview time makes the model slightly unrealistic. | Single feedback form | <p style="text-align: center;">FIG. 4. Linear system representation.</p> |
| 1977 | STI [37] | 3 | Concern: no preview incorporated in this model. Pro: it includes open-loop compensation of the lateral position error and heading error. | Open-loop feedforward control of the road curvature and closed-loop compensation of the lateral position error and heading error. Also includes feedback paths. | <p style="text-align: center;">FIG. 2. Preview-predictor model structure</p> |
| 1978 | Donges Two-Level [9] | 4 | The curvature feedback, although enhancing performance slightly, causes high frequency oscillations in the steering behavior at higher gains, which is not very realistic behavior. Due to the four inputs identification of the two-level model PRF's will be very difficult or impossible, and consequently the parameters in the model cannot be obtained. Uses linear optimal control theory to feedback corrective forces to get to the optimal steering angle so that there is a minimal future path error | Anticipatory open-loop control and compensatory closed-loop control | <p style="text-align: center;">FIG. 3. Block diagram for the single-point preview control.</p> |
| 1981 | Optimal Preview Control [38] | 1-∞ | Due to its complexity and the large number of preview points it is relatively difficult to execute identification of human driver for optimal preview models | Single feedback loop | <p style="text-align: center;">FIG. 1. Overview of the autonomous vehicle control using driver model</p> |
| 1981 | Optimal Preview Acceleration [9] | 1-∞ | Due to its complexity and the large number of preview points it is relatively difficult to execute identification of human driver for optimal preview models | One feedback loop | <p style="text-align: center;">FIG. 1. Overview of the autonomous vehicle control using driver model</p> |

| Date | Driver Model | Inputs | Limitations & Boundaries | Feedback & Feedforward Multiple loops | Module structure |
|------|------------------------------------|--------|--|---------------------------------------|------------------|
| 1990 | Hess[30] | 1 | Only uses lateral error as input making the model less realistic | 1 feedback loop | |
| 2009 | Sentouh's Two-Point [11] | 3 | A big advantage of using the visual angle over the predicted error is that there is no more dependency on a fixed preview time nor on velocity in the driver model. Drawback of using the visual angle is that the observation behavior must be modeled as well. Most importantly, it must be known when drivers start looking at the tangent point and start using this far-angle for control. | Single feedback loop | |
| 2011 | Adapted Two-Point | 2 | With this new set-up of the two-point model, the anticipatory control is proportional to the actual curvature resulting in much more realistic driving behavior. This way the anticipatory gain, can be used to tune the corner cutting behavior. A high gain will result in severe corner cutting, which will be increasing with the sharpness of a curve, contrary to the behavior displayed by Sentouh's two-point model. Another advantage is that with this corner cutting behavior, the short curve behavior improves as well. When the driver cuts the corners, the vehicle will be closer to the inner lane boundary. This results in a lower estimate of the curvature, because the visual angle to the tangent point decreases; balancing out the over steering. Model based on the guidance level of the forcing function of the future path and the stabilization level to take on sudden deviations in closed-loop control. A concern is however that the results showed a high dependency on the experimental test conditions. | Feedback control | |
| 2013 | Two-Level Cooperative Control [39] | 2 | | Feedback control | |
| 2016 | Stochastic Model Prediction | 3 | Numerous gains by which it is difficult to see what is going on making the model relatively complex for further research | Single feedback loop | |

Bibliography

- [1] Jean-Michel Hoc (2000) *From human – machine interaction to human – machine co-operation*, Ergonomics, 43:7, 833-843, DOI: 10.1080/001401300409044
- [2] Lappi O., Lehtonen E., Pekkanen J. & Itkamen T.(2013). *Beyond the tangent point: gaze targets in naturalistic driving*. Journal of Vision, Helsinki, 13(13):11, 1-18, <http://www.journalofvision.org/content/13/13/11>, DOI:10.1167/13.13.11.
- [3] Mars F. (2008). *Driving around bends with manipulated eye-steering coordination*. Journal of Vision, STAD, 8(11):10, 1–11, <http://journalofvision.org/8/11/10/>, DOI: 10.1167/8.11.10.
- [4] Bosetti P., Da Lio M., Saroldi A.(2015). *On curve negotiation: from driver support to automation*. IEEE Transactions on Intelligent Transportation Systems, <http://ieeexplore.ieee.org/stamp/stamp.jsp?arnumber=7045558>
- [5] Nash C.J., Cole D.J., Bigler R.S. (2016). *A review of human sensory dynamics for applications to models of driver steering and speed control*. Biological Cybernetics, <http://link.springer.com/10.1007/s00422-016-0682-x>
- [6] Odhams A., Cole D. (2004). *Models of driver speed choice in curves*. 7th International Symposium on Advanced Vehicle Control (AVEC 04), [http : //www2.eng.cam.ac.uk/ djc13/vehicledynamics/downloads/OdhamsCole_AVEC2004.pdf](http://www2.eng.cam.ac.uk/djc13/vehicledynamics/downloads/OdhamsCole_AVEC2004.pdf)
- [7] Levison W. (2007) *Development of a drive vehicle module for the interactive highway safety design model*. Fhwa-Hrt-08-019, <http://trb.metapress.com/index/E502737105126817.pdf>
- [8] Saleh L., Chevrel P., Claveau F, et al. (2013). *Shared steering control between a driver and an automation: stability in the presence of driver behavior uncertainty*. IEEE Transactions on Intelligent Transportation Systems, DOI: 10.1109/TITS.2013.2248363
- [9] Steen J., Damveld H., Happee R., et al. (2011). *A review of visual driver models for system identification purposes*. Conference Proceedings - IEEE International Conference on Systems, Man and Cybernetics, DOI: 10.1109/ICSMC.2011.6083981

- [10] Keen S., Cole D. (2012). *Bias-free identification of a linear model-predictive steering controller from measured driver steering behavior*. IEEE Transactions on Systems, Man, and Cybernetics, Part B: Cybernetics, DOI: 10.1109/TSMCB.2011.2167509
- [11] Sentouh C., Chevrel P., Mars F., et al. (2009). *A sensorimotor driver model for steering control*. Conference Proceedings - IEEE International Conference on Systems, Man and Cybernetics, DOI: 10.1109/ICSMC.2009.5346350
- [12] Okuda H., Ikami N., Suzuki T. (2012). *Modeling and analysis of driving behavior based on a probability-weighted ARX model*. IEEE Transactions on Intelligent Transportation Systems, <http://ieeexplore.ieee.org/stamp/stamp.jsp?arnumber=6256731>
- [13] Qu T., Chen H., Ji Y., et al. (2013). *A stochastic model predictive control approach for modeling human driver steering control*. 2013 International Conference on Systems, Man, and Cybernetics (SMC), DOI: 10.1109/SMC.2013.631
- [14] Soualmi B., Sentouh C., Popieui J., et al. (2013). *Cooperative steering assist control system*. 2013 International Conference on Systems, Man, and Cybernetics (SMC), DOI: 10.1109/SMC.2013.165
- [15] Salvucci D. D. (2006). *Modeling driver behavior in a cognitive architecture*. Human Factors, DOI: 10.1518/001872006777724417
- [16] Land M., Lee D. (1994). *Where we look when we steer*. Nature, 369, 742–744.
- [17] Lappi O. Pekkanen J. Itkonen T. (2013). *Pursuit eye-movements in curve driving differentiate between future path and tangent point models*. PLoS ONE, 8 (7), e68326.
- [18] Qu T., Chen H., Ji Y., Guo H., Xu Y. (2016). *A stochastic model predictive control approach for modelling human driver steering control*. Int. J. Vehicle Design, Vol. 70, No. 3, pp.249-277
- [19] Dong Y., Hu Z. (2011). *Driver Inattention Monitoring System for Intelligent Vehicles: A Review*. IEEE, Vol. 12, No. 2, 2011
- [20] Boink R., van Paassen R., Mulder M., Abbink D. (2014). *Understanding and reducing conflicts between driver and haptic shared control*. IEEE, DOI: 10.1109/SMC.2014.6974130
- [21] van Paassen R., Boink R., Abbink D., Mulder M., Mulder M. (2016). *Haptic guidance, interaction between the guidance model and tuning* not yet published
- [22] Lehtonen E. Lappi O. Summala H. (2012). *Anticipatory eye movements when approaching a curve on a rural road depend on working memory load*. Transportation Research Part F, 15, 369-377.

- [23] Wyzen P., Paassen van M.M., Abbink D.A. (2017). *Separating Haptic Guidance and Support Signals: a Solution for Human-Machine Cooperation?*. Delft University of Technology
- [24] Salvucci D., Gray R. (2004). *A Two-Point Visual Control Model of Steering Perception*
- [25] Michon J. (1985). *A Critical View of Driver Behavior Models: What Do We Know, What Should We Do?* Human Behavior & Traffic Society, 1985
- [26] Lewis-Evans B., Charlton S. (2005). *Explicit and implicit processes in behavioural adaptation to road width* Accident Analysis & Prevention, Elsevier, May 2006
- [27] Reymond G., Kemeny A., Droulez J., Berthoz A. (2001). *Role of Lateral Acceleration in Curve Driving: Driver Model and Experiments on a Real Vehicle and a Driving Simulator* Human Factors, Vol. 43, No. 3, Fall 2001, pp. 483-495
- [28] Abbink D.A., Mulder M. (2010). *Neuromuscular Analysis as a Guideline in designing Shared Control* www.intechopen.com
- [29] Abbink D.A., Mulder M. (2009). *Relating biodynamic feedthrough to neuromuscular admittance* 2009 IEEE International Conference on Systems, Man, and Cybernetics pp. 1730–1735
- [30] Hess R., Modjtahedzadeh A. (1990). *A Control Theoretic Model of Driver Steering Behavior* IEEE Control Systems Magazine
- [31] Kondo M., Ajimine A. 1968. *Driver's Sight Point and Dynamics of the Driver-Vehicle-System Related to It* SAE Paper, no. 680104, 1968
- [32] Van Winsum W., Godthelp J. (1996). *Speed choice and steering behavior in curve driving* Human Factors and Ergonomics Society Inc.
- [33] Spacek P. (2005). *Track Behavior in Curve Areas: an Attempt at Typology* Journal of transportation engineering
- [34] Beall A.C., Loomis J.M. (1996). *Visual control of steering without course information* Perception, volume 25, page 481-494
- [35] Boer E.R. (1996). *Tangent point oriented curve negotiation* Proceedings of the 1996 IEEE Intelligent Vehicles Symposium (pp. 7–12). Tokyo: Japan.
- [36] McRuer D.T. (1959). *The human operator as a servo system element* Journal of the Franklin Institute 267(6):511-536
- [37] McRuer D.T. (1977) *New results in driver steering control models*

- [38] MacAdam C.C. (1980) *An optimal preview control for linear systems* Journal of dynamic systems measurement and control 102(3)
- [39] Donges E. (1978) *A two-level model of driver steering behavior* Human Factors The Journal of the Human Factory and Ergonomics Society 20(6):691-707

Appendix B

Inherent identifiability of the nonlinear model

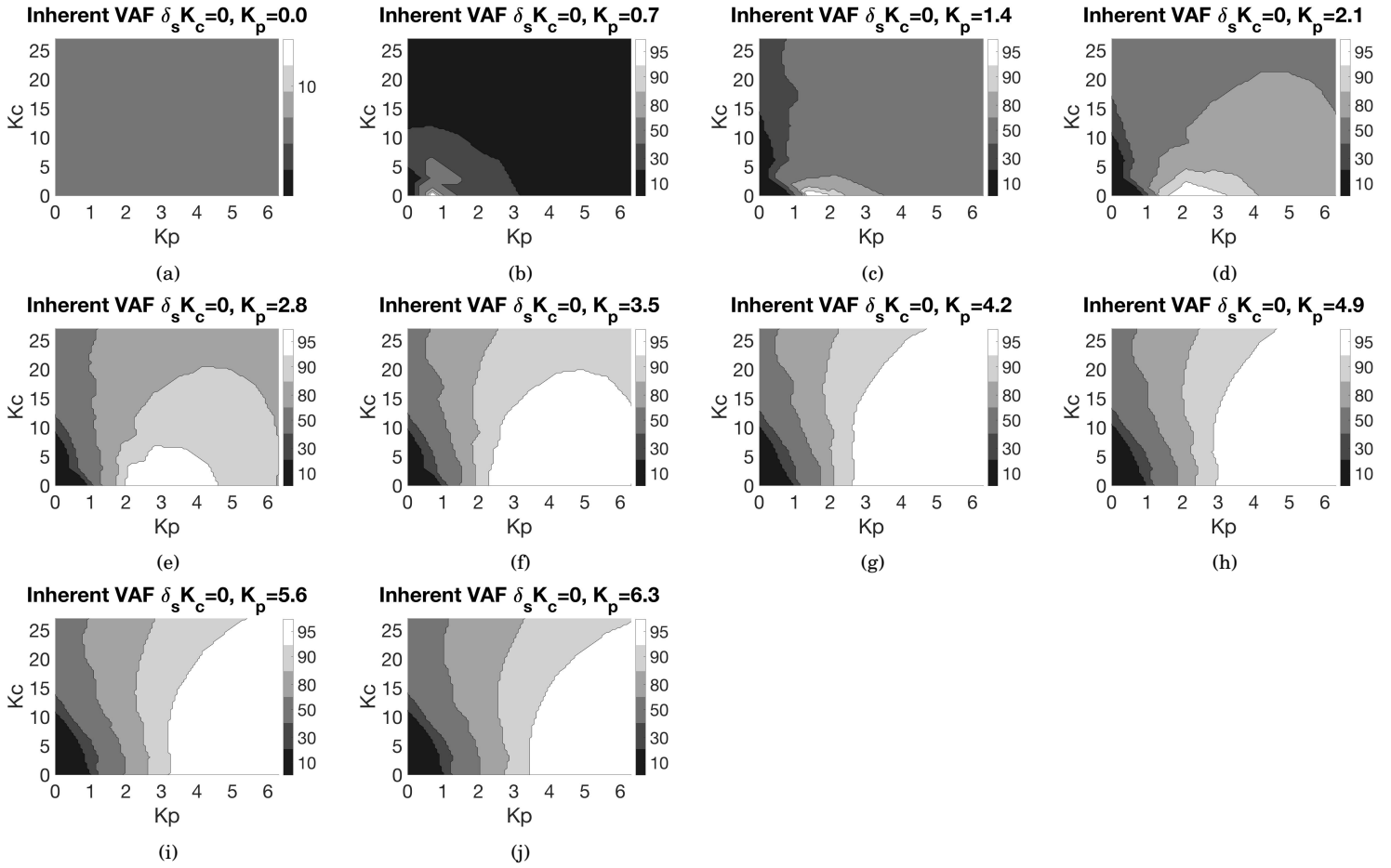


Figure 1: Variance Accounted for Inherent Steering Wheel Angle $K_c=0$, Nonlinear model

The inherent identifiability of the nonlinear model has been analyzed over the full set of K_c (0-27) and K_p (0-6.3). All runs, where an array of data with a specific K_c and K_p value is compared to the entire data set, are shown in figures 2a to 20j. The right y-axis depicts the percentage of how well the array of data overlaps with the whole matrix set of data.

Looking at the variance accounted for for the steering wheel angle, it is clear to see the largest area of 95 to 100 % is found at the K_c and K_p values lying closest to the centre of the data matrix, as well as falling in the realism bound. This can be explained by the fact that the realistic combinations are able to describe other combinations better due to their more stable data. Combinations which lie outside of the realism bound, show more extreme data, with heavier jitters and out of position bounds driving behaviour. This results in a worse identifiability mapping due to the more 'unique' behaviour of a out-lier combination of K_c and K_p .

When looking at the variance accounted for for lateral position, we do not necessarily see the same increase in high percentage area as with the lateral position. The area of 'identifiable' combinations merely shift its position in the VAF graph, mirroring the K_c and K_p value of the analyzed array of data. The lateral position mapping is more sensitive to the chosen parameter values than the steering wheel angle mapping is. This effect can also be seen in a more extreme way in the experimental identifiability in figures 21 and 22 where, when looking at the VAF in both left and right curves, the experimental identifiability can't even reach 5%. This can be explained by the fact that the car has a wide lateral position range where it drives safe on the road in the range from 0 to 3.6 meter, when maintaining an average logical steering wheel angle. It is much harder to deviate far from the steering wheel angle, without maintaining the curvature of the road.

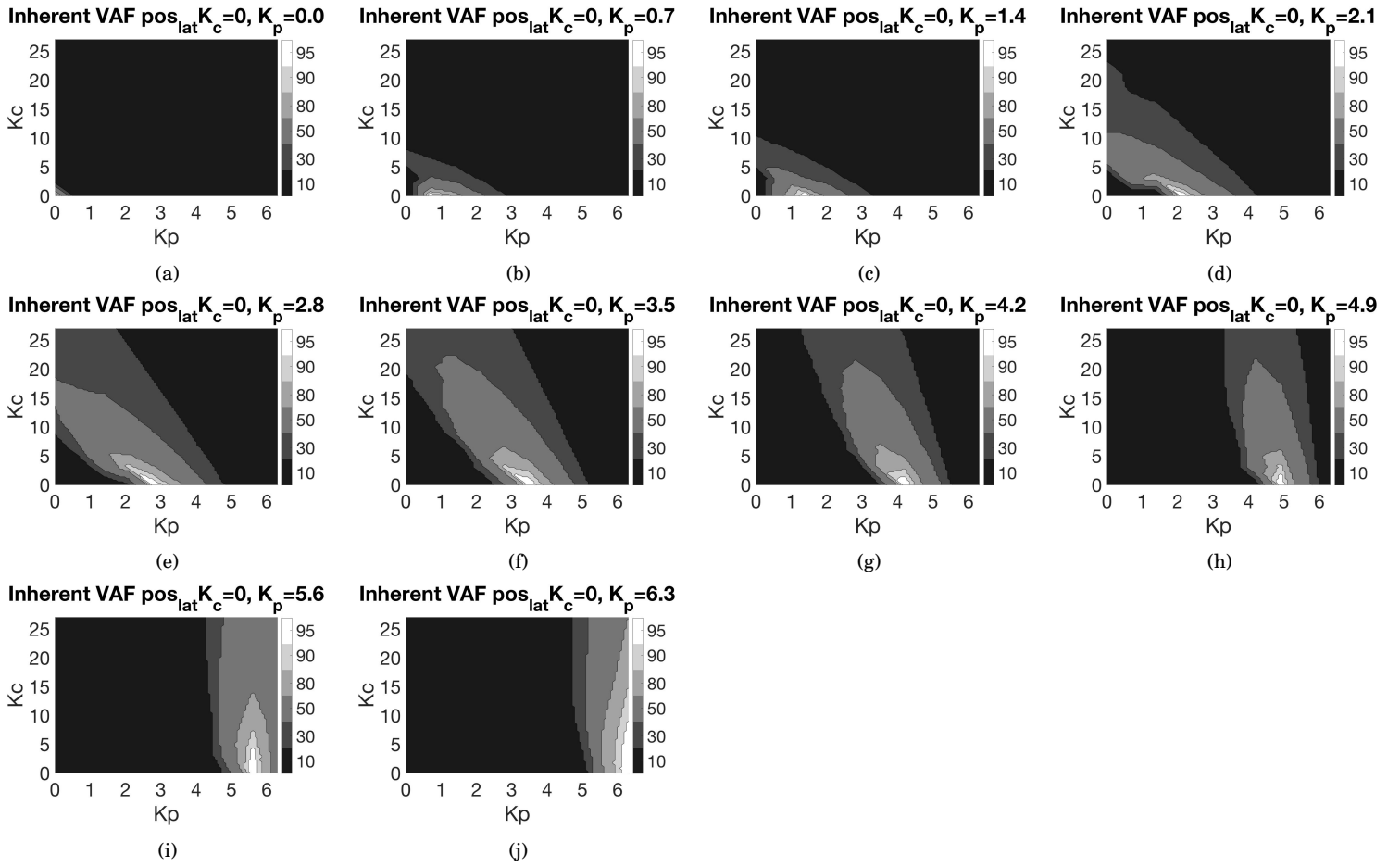


Figure 2: Variance Accounted for Inherent Lateral Position $K_c=0$, Nonlinear model

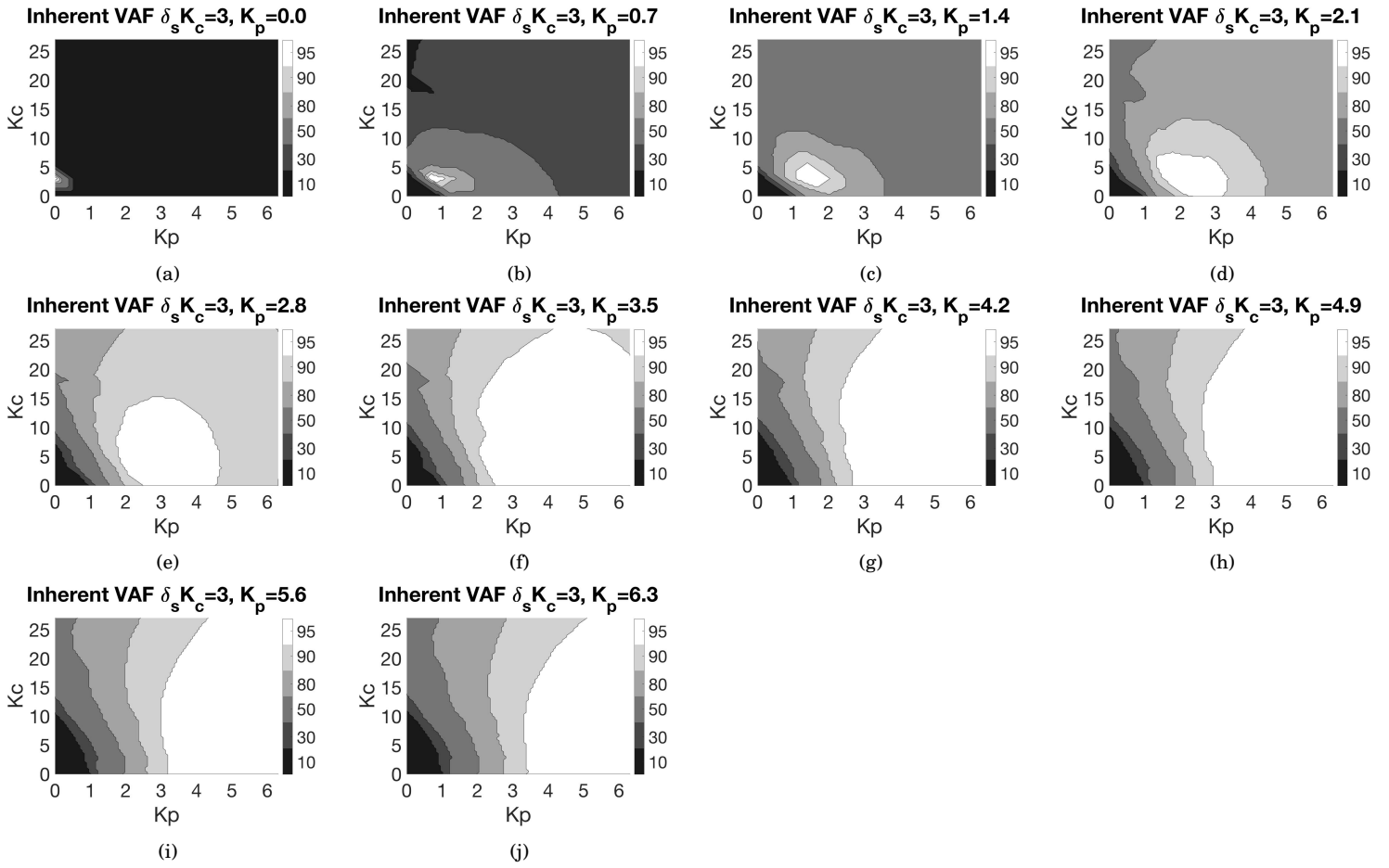


Figure 3: Variance Accounted for Inherent Steering Wheel Angle $K_c=3$, Nonlinear model

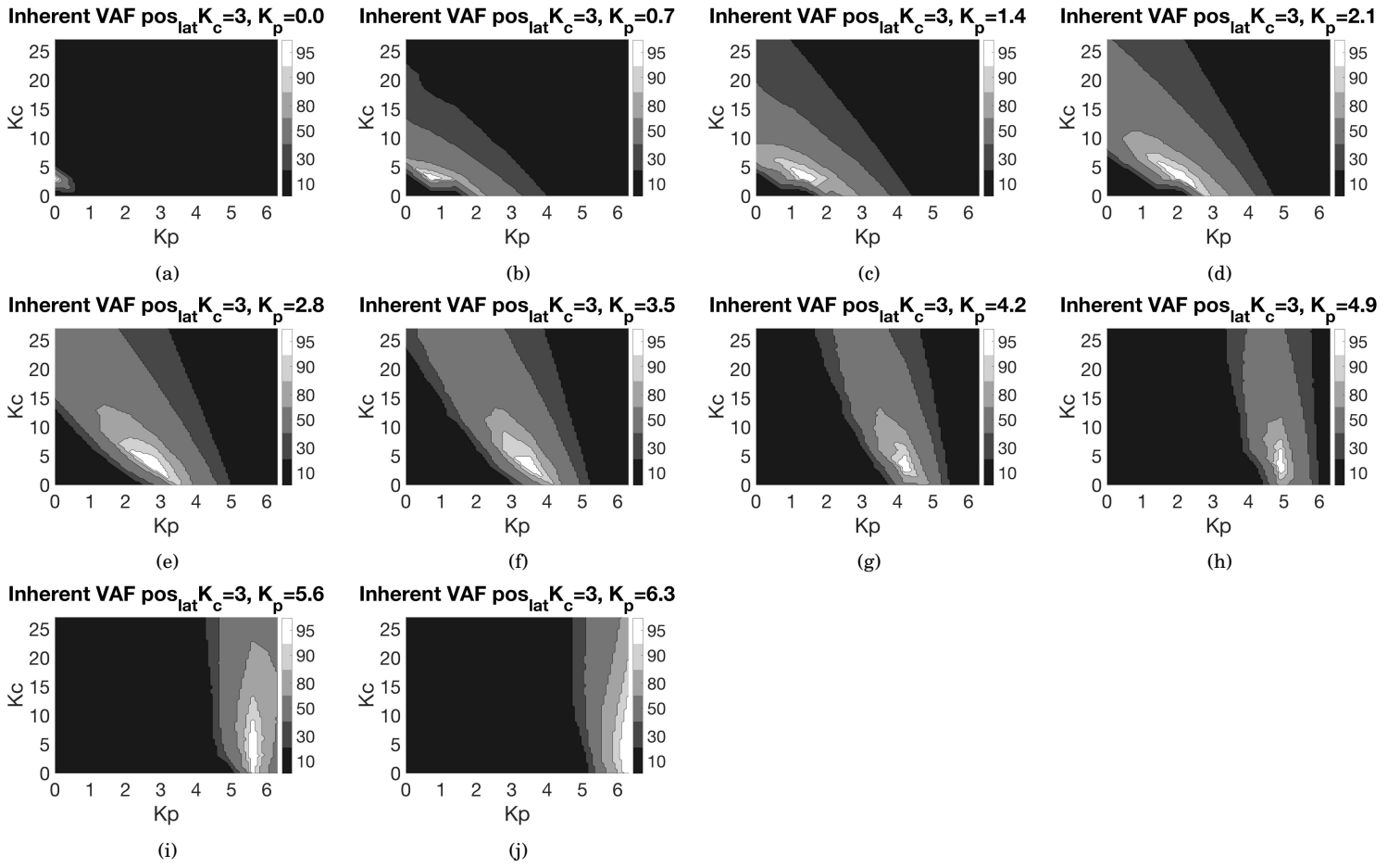


Figure 4: Variance Accounted for Inherent Lateral Position $K_c=3$, Nonlinear model

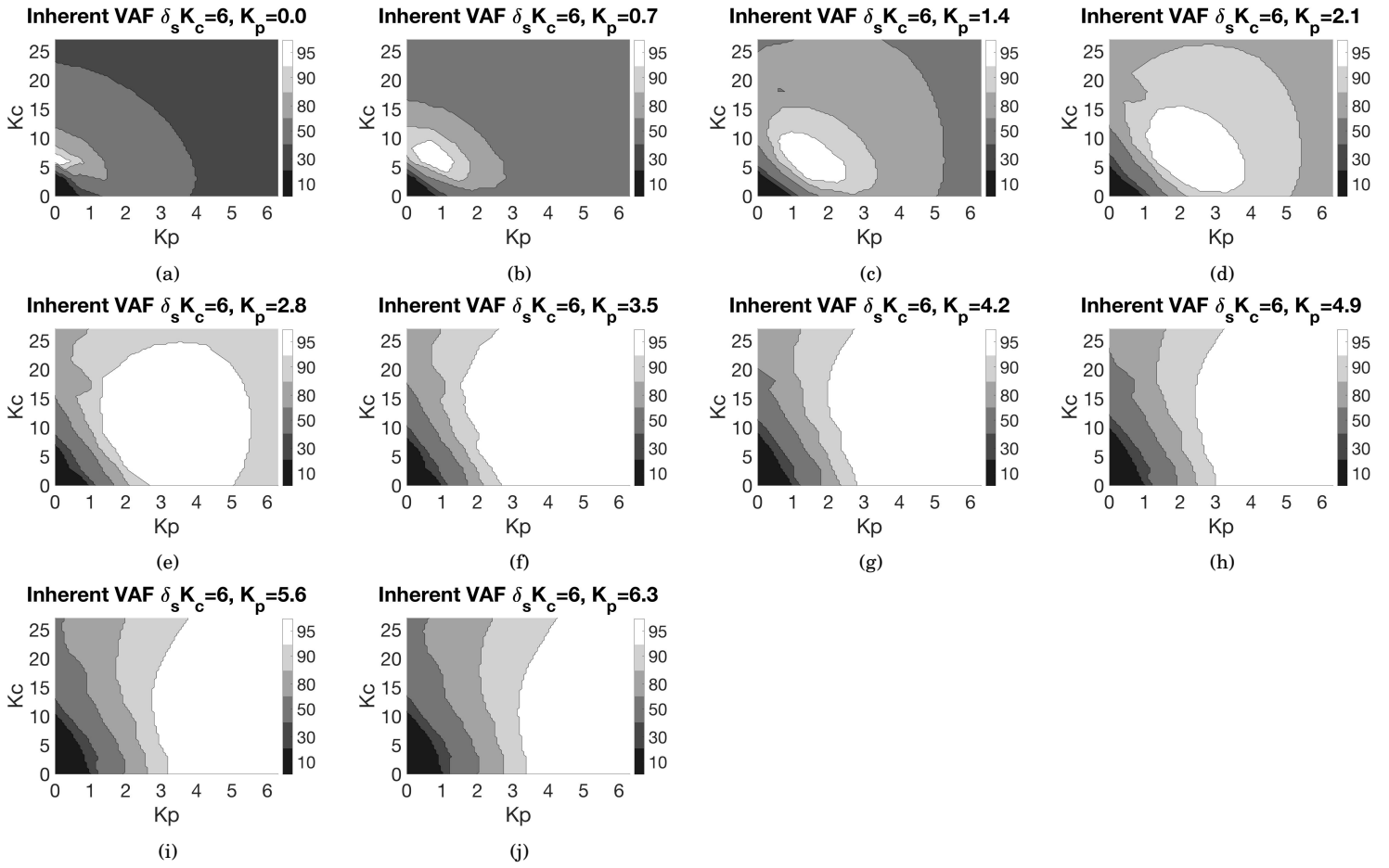


Figure 5: Variance Accounted for Inherent Steering Wheel Angle $K_c=6$, Nonlinear model

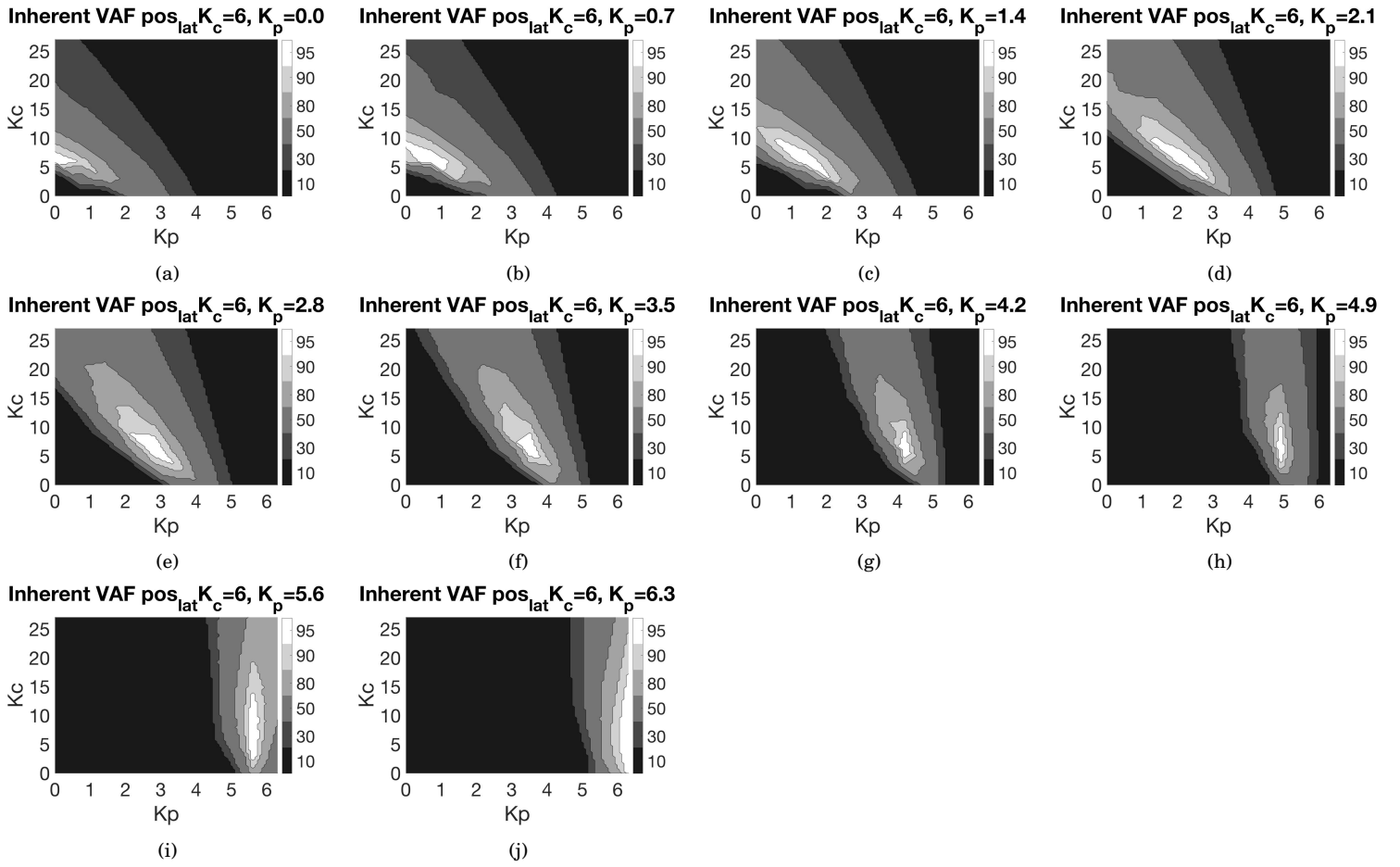


Figure 6: Variance Accounted for Inherent Lateral Position $K_c=6$, Nonlinear model

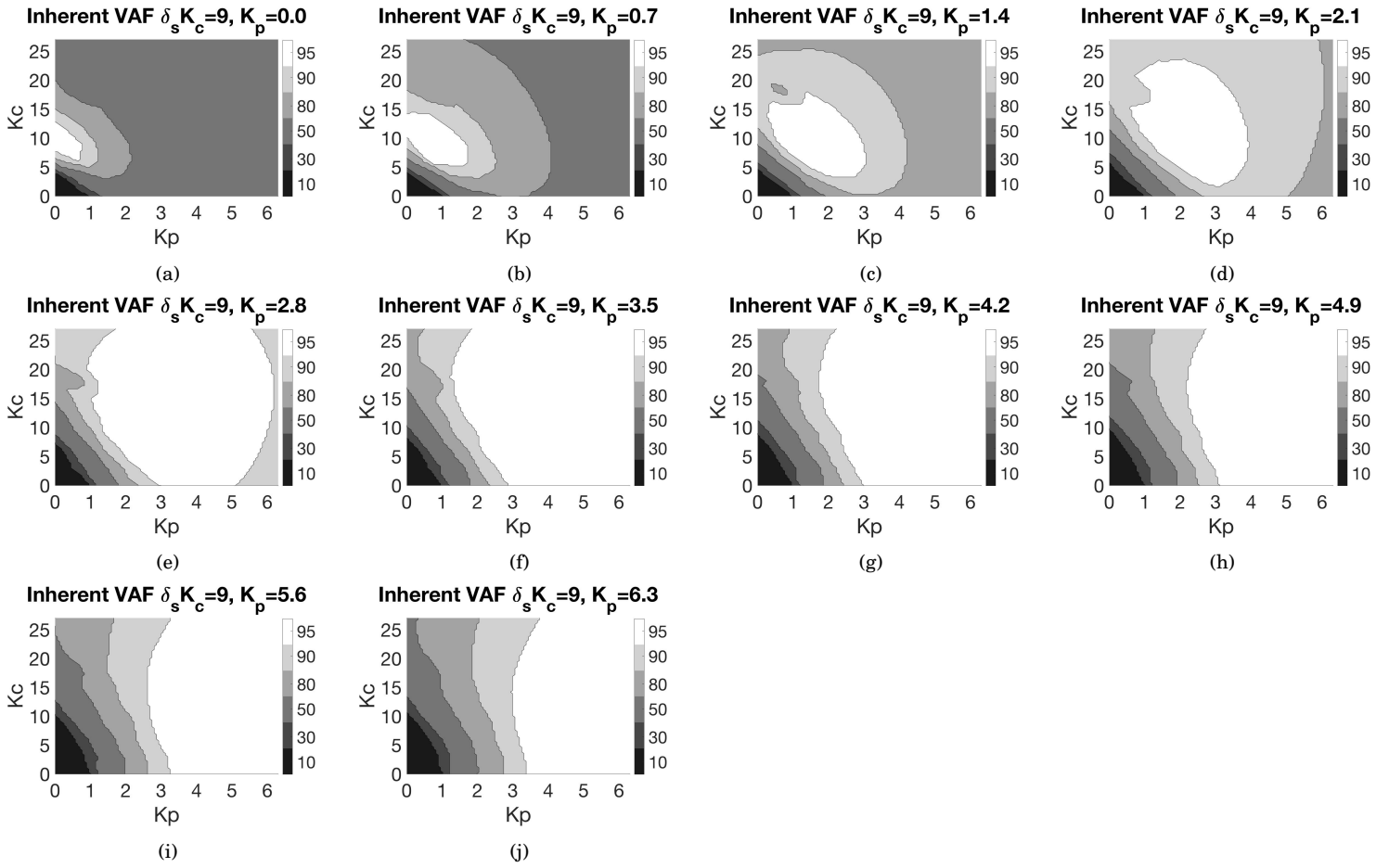


Figure 7: Variance Accounted for Inherent Steering Wheel Angle $K_c=9$, Nonlinear model

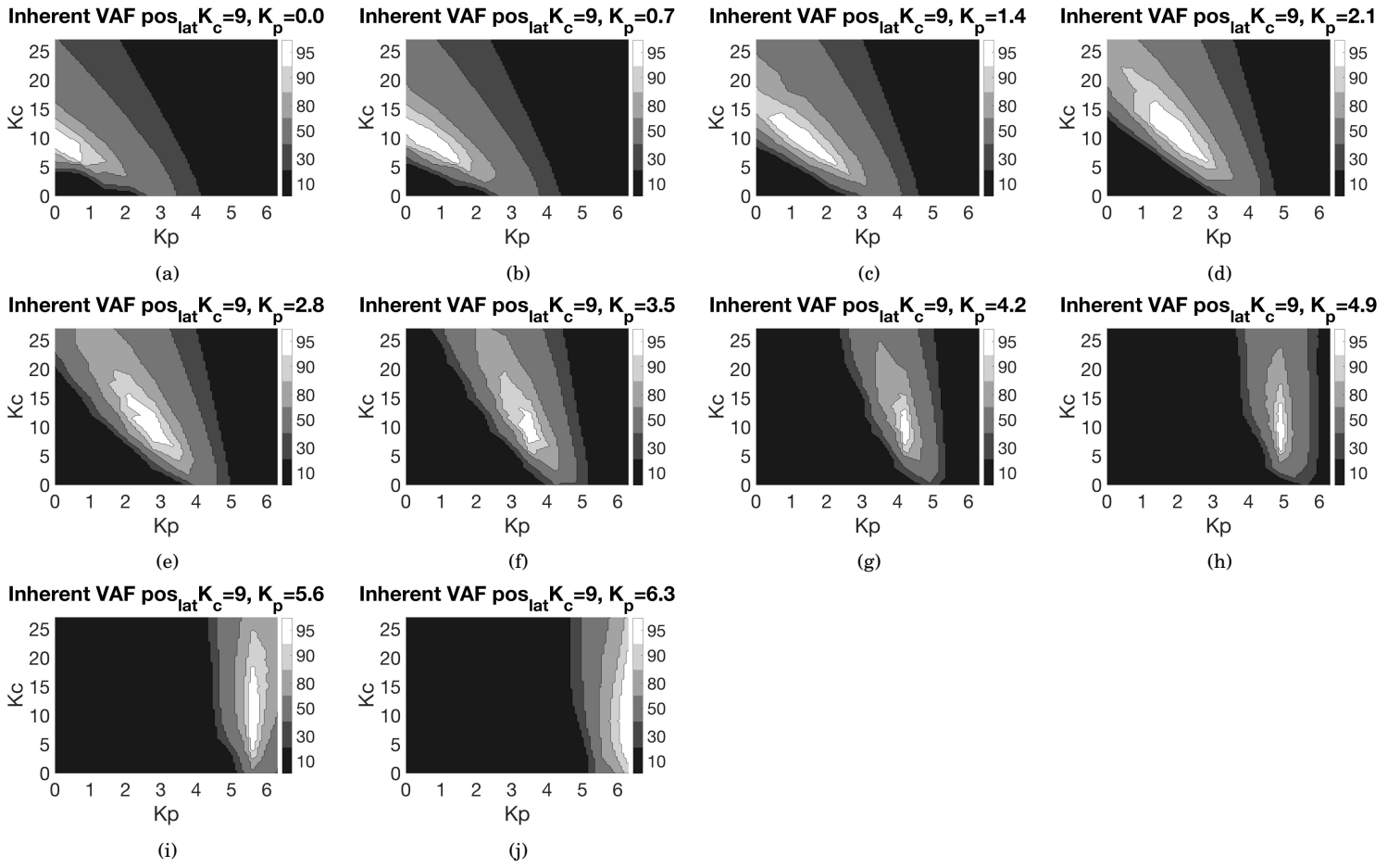


Figure 8: Variance Accounted for Inherent Lateral Position $K_c=9$, Nonlinear model

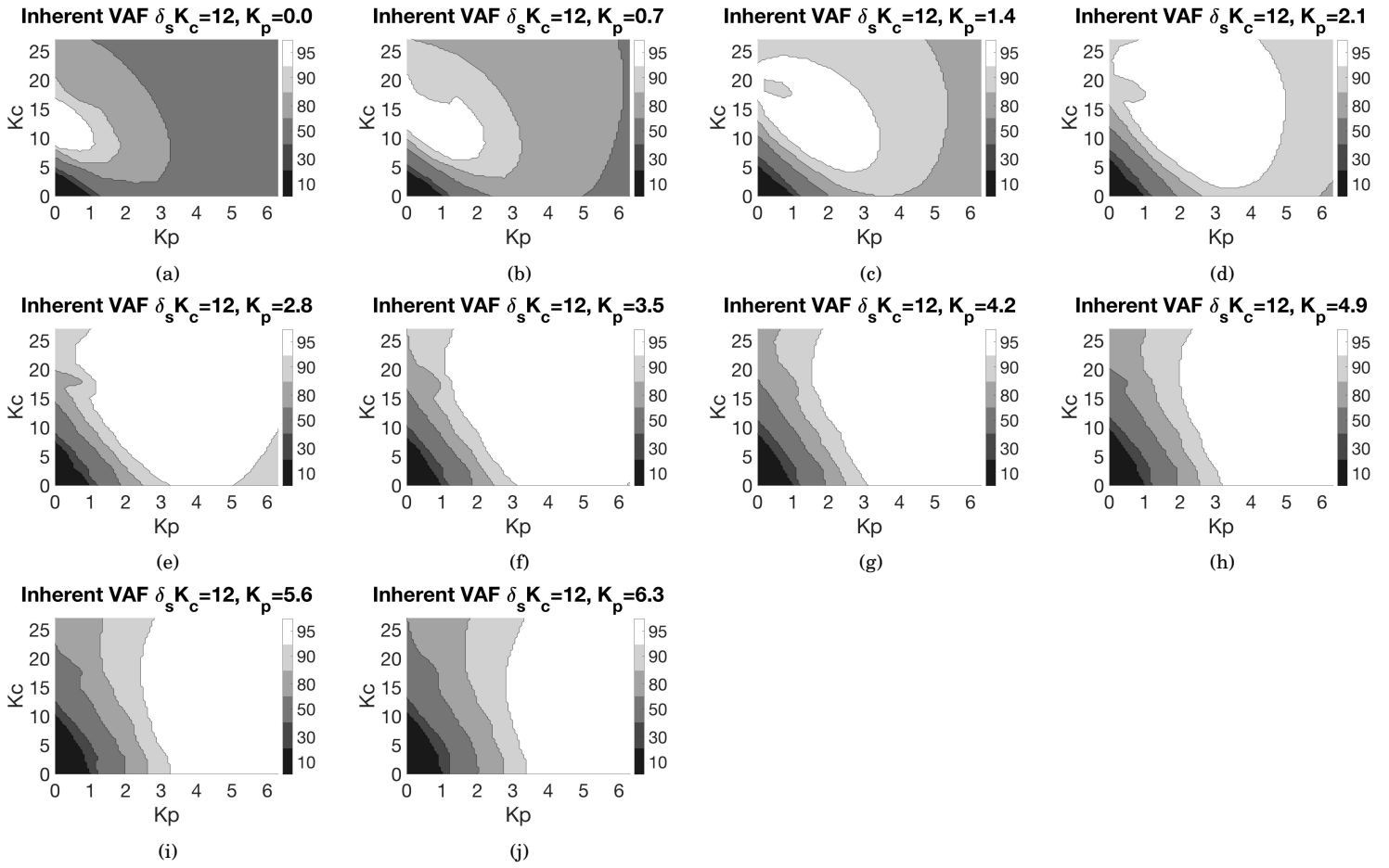


Figure 9: Variance Accounted for Inherent Steering Wheel Angle $K_c=12$, Nonlinear model

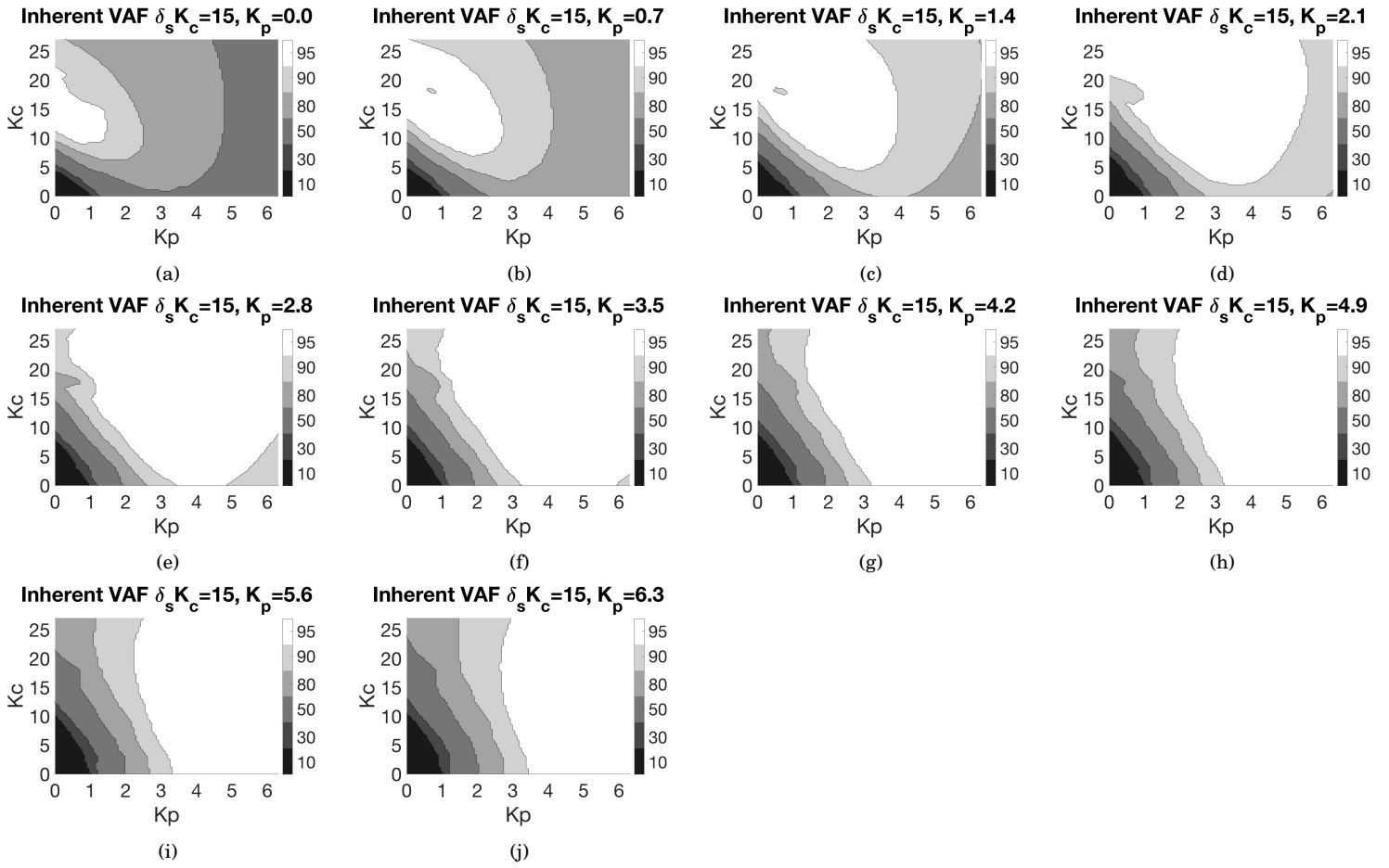


Figure 11: Variance Accounted for Inherent Steering Wheel Angle $K_c=15$, Nonlinear model

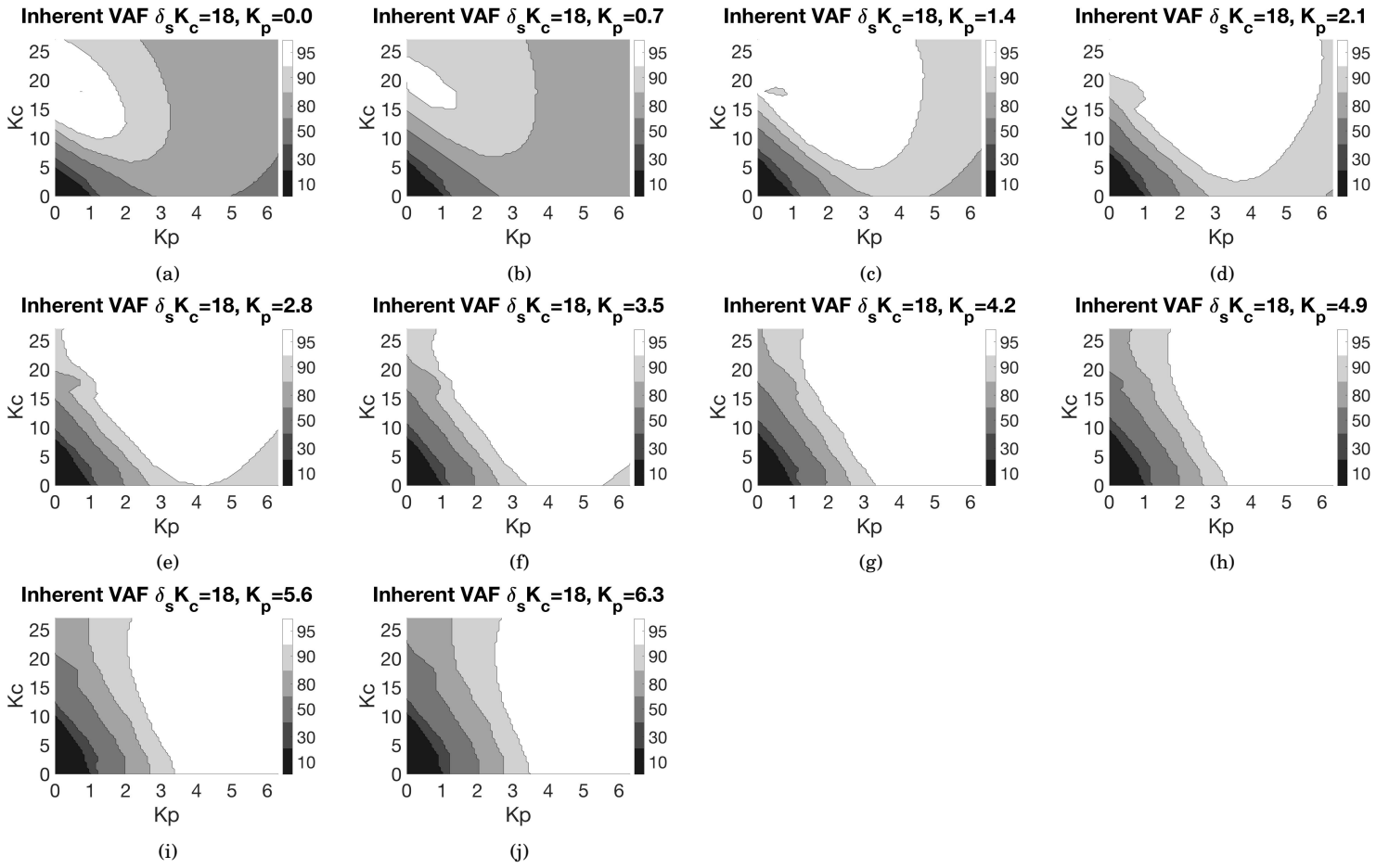


Figure 13: Variance Accounted for Inherent Steering Wheel Angle $K_c=18$, Nonlinear model

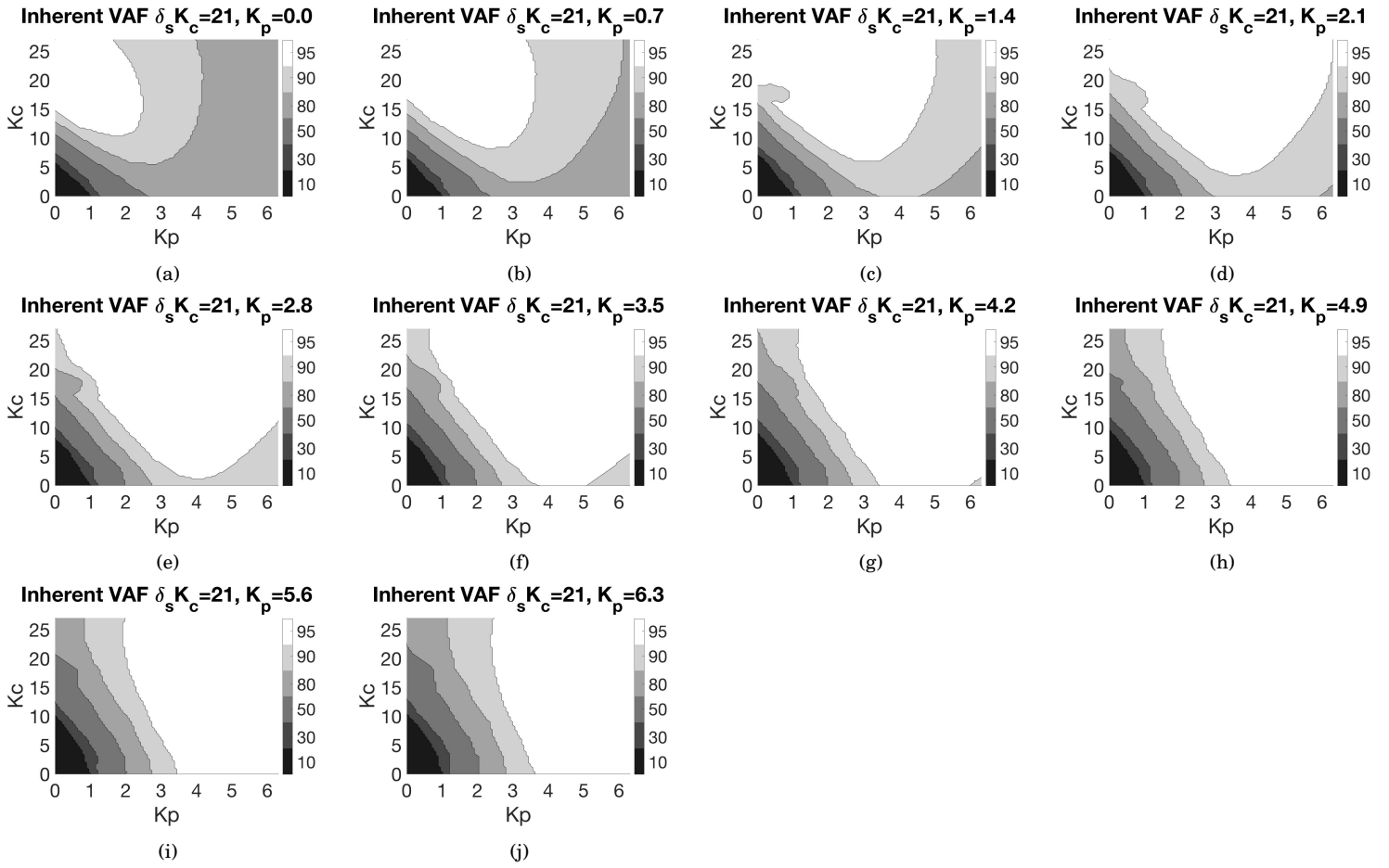


Figure 15: Variance Accounted for Inherent Steering Wheel Angle $K_c=21$, Nonlinear model

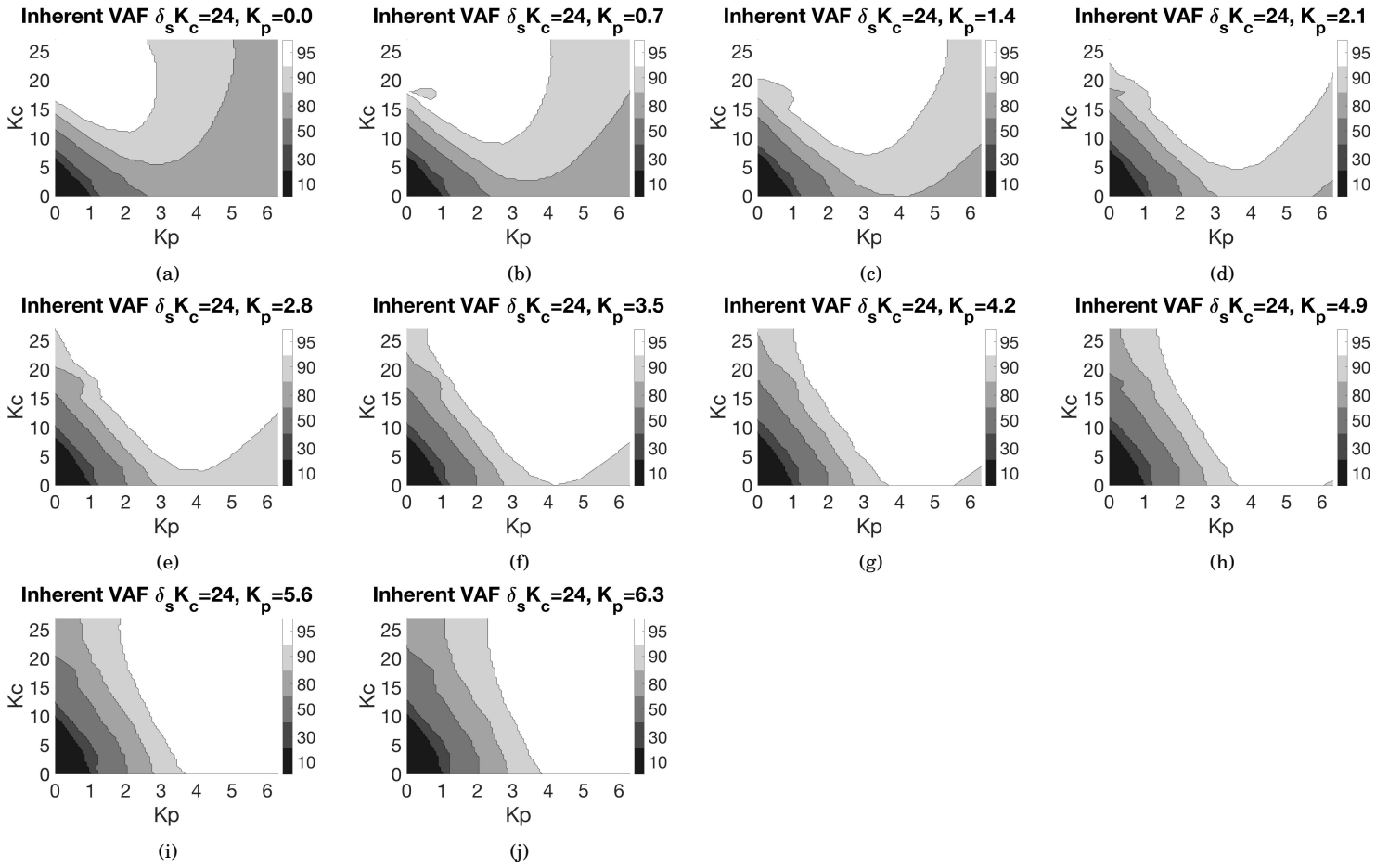


Figure 17: Variance Accounted for Inherent Steering Wheel Angle $K_c=24$, Nonlinear model

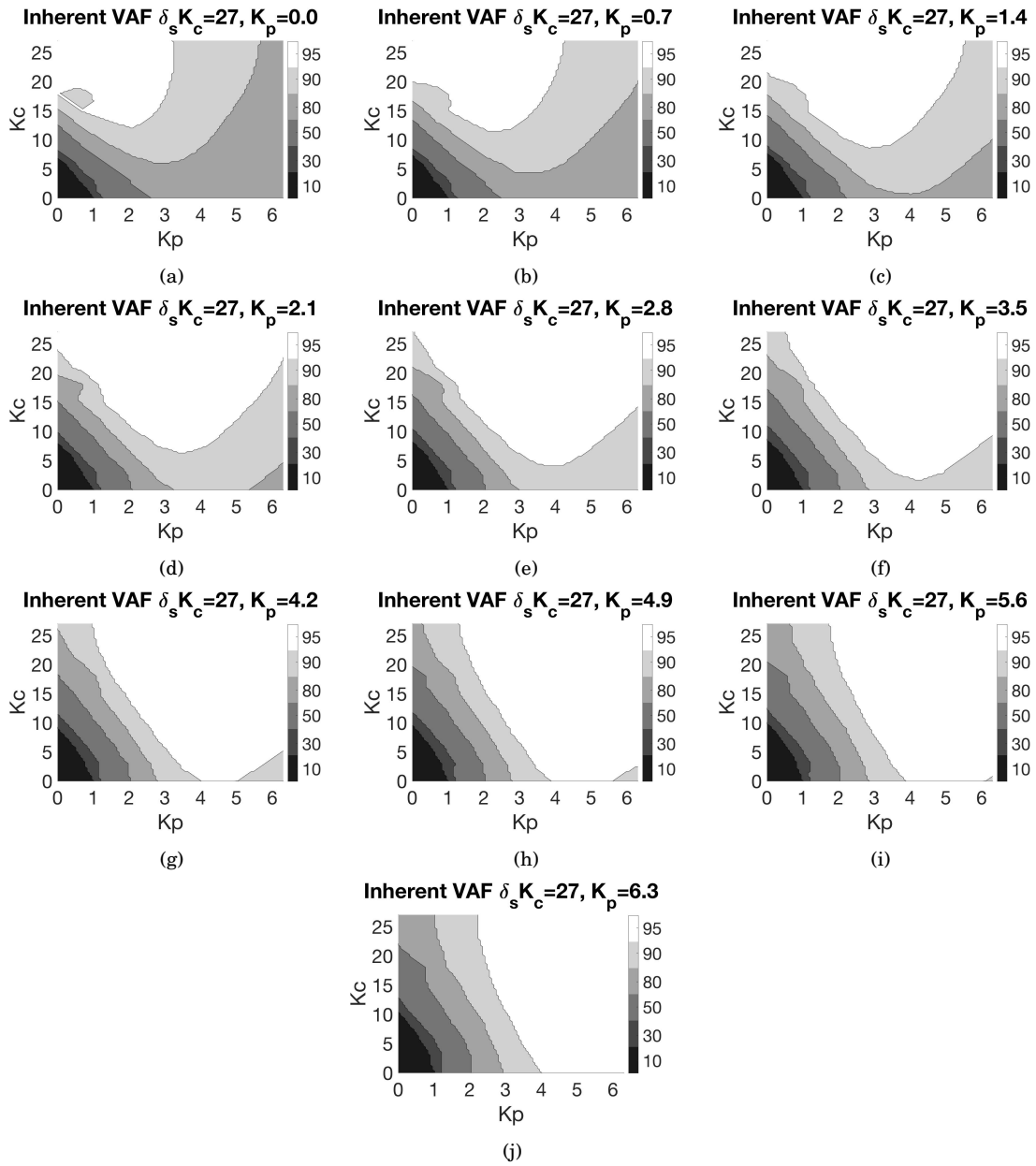


Figure 19: Variance Accounted for Inherent Steering Wheel Angle $K_c=27$, Nonlinear model

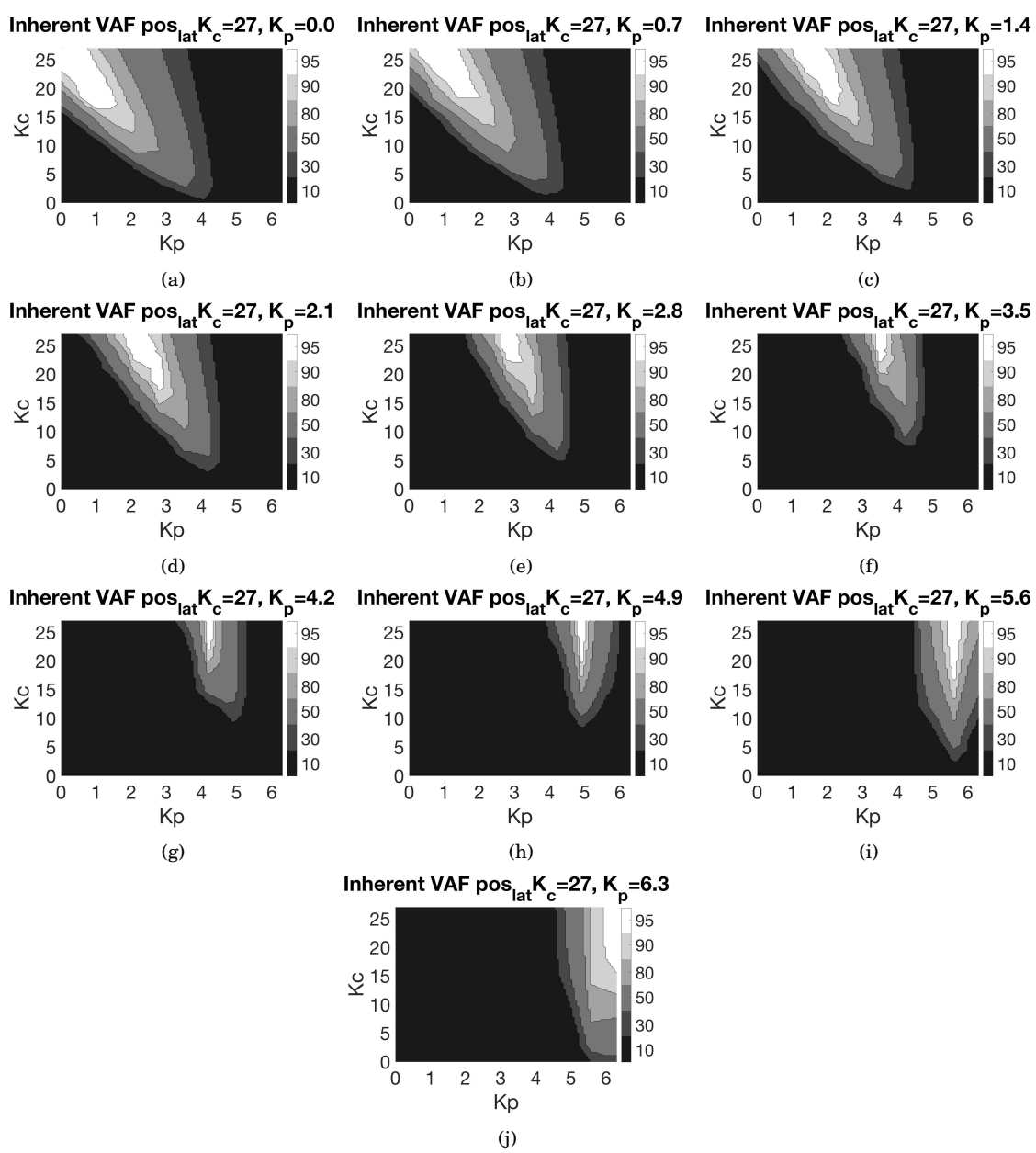


Figure 20: Variance Accounted for Inherent Lateral Position $K_c=27$, Nonlinear model

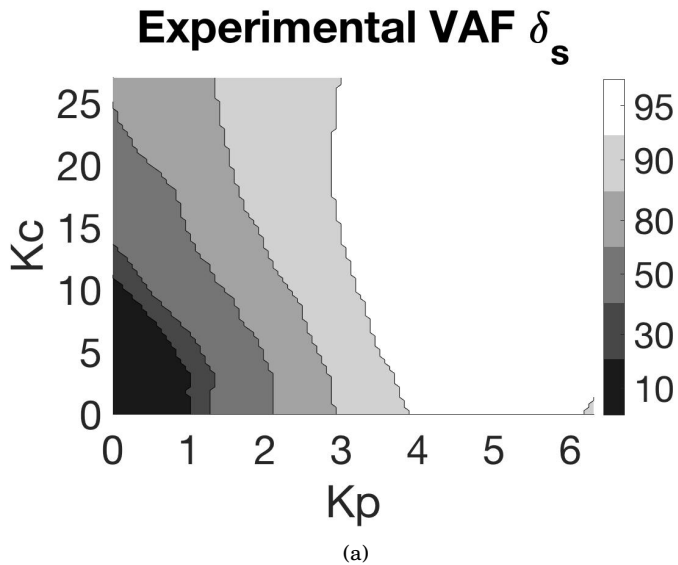


Figure 21: Variance Accounted for Experimental Steering Wheel Angle, nonlinear model

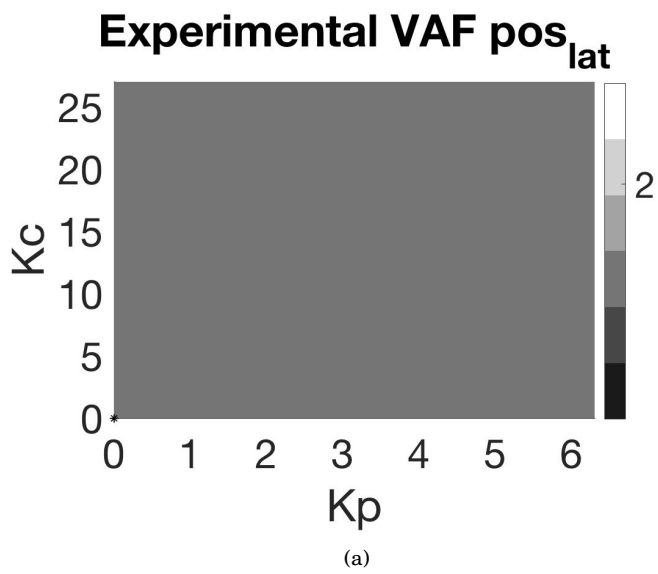


Figure 22: Variance Accounted for Experimental Lateral Position, nonlinear model

Appendix C

Inherent identifiability of the linear model

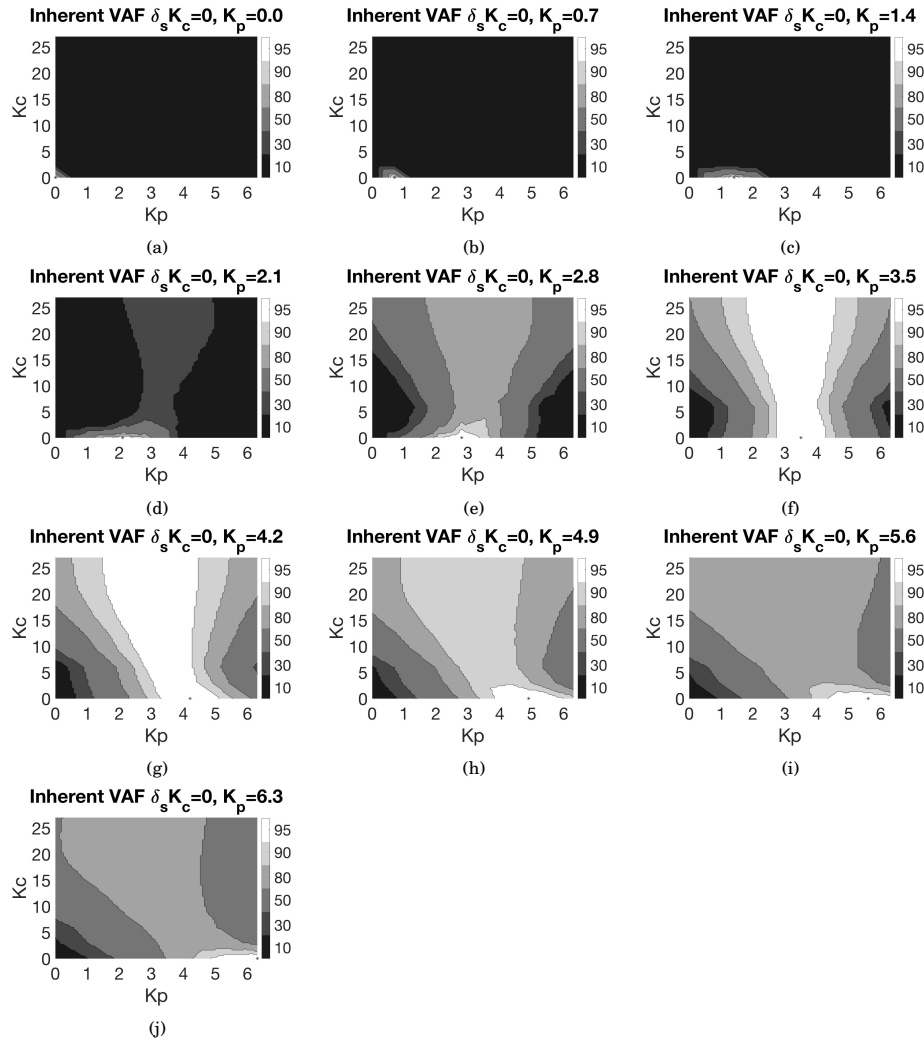


Figure 1: Variance Accounted for Inherent Steering Wheel Angle $K_c=0$, Linear model

Figures 1 to 20 show the inherent identifiability for the linear model. The left y-axis shows the K_c value and the x-axis the K_p value. The right y-axis shows the percentage of variance accounted for (VAF), when comparing the specific K_c and K_p data-array with the entire data matrix.

Figure 21 shows the experimental identifiability for the linear model with the output steering wheel angle and lateral position. The high percentage level area (above 90%), shows to be significantly smaller compared to the nonlinear model identifiability. This can be seen in both outputs, the steering wheel angle and the lateral position. This also came forward in one of the conclusions of the article, that the linear model is therefore more sensitive to a change in parameter value of K_c or K_p .

The experimental identifiability (figure 21) shows a low VAF for the lateral position, which coincides with the nonlinear experimental identifiability of the lateral position. Due to the different curve driving in left and right curves, the model was not capable to describe the driving behaviour in left curves as well as in the right curves, which resulted in the bad VAF values. This is less of an issue when looking at the VAF of the steering wheel angle because, even though a driver can be curve cutting or over steering, the steering wheel angle will still have to follow the curvature of the road.

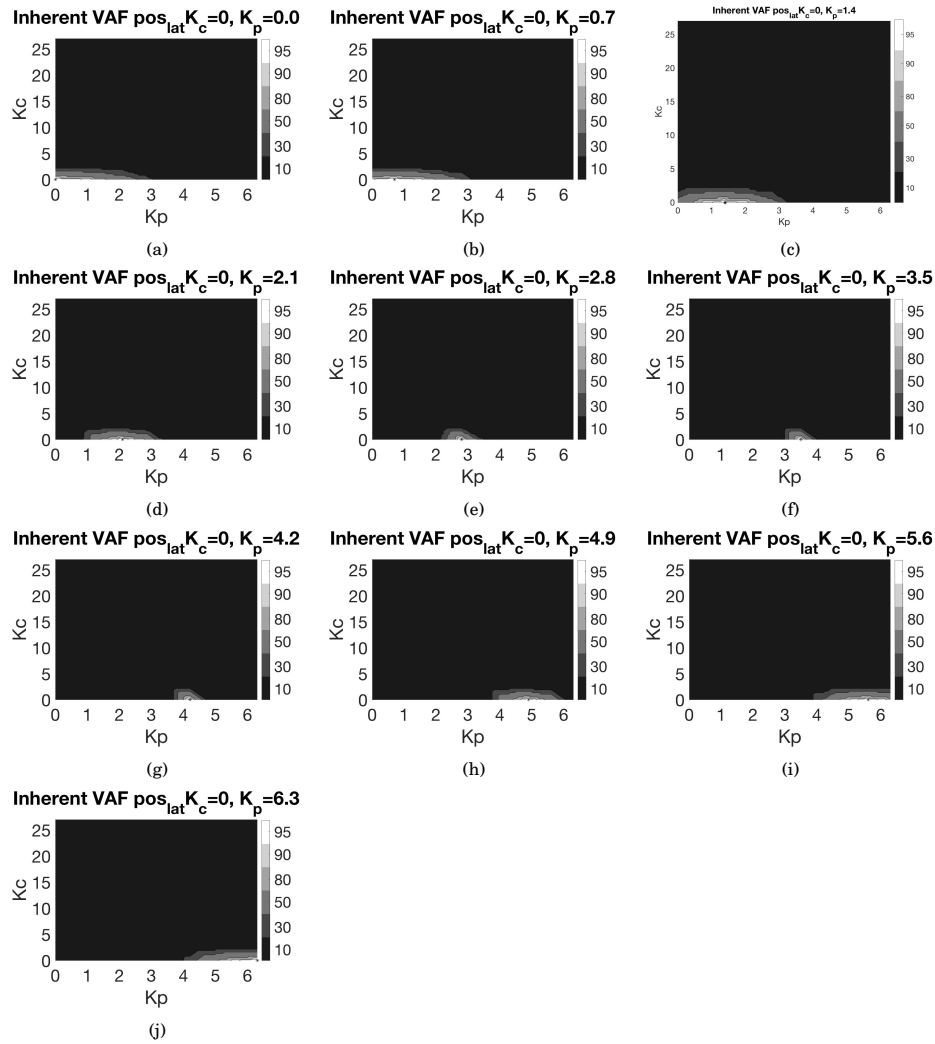


Figure 2: Variance Accounted for Inherent Steering Wheel Angle $K_c=0$, Linear model

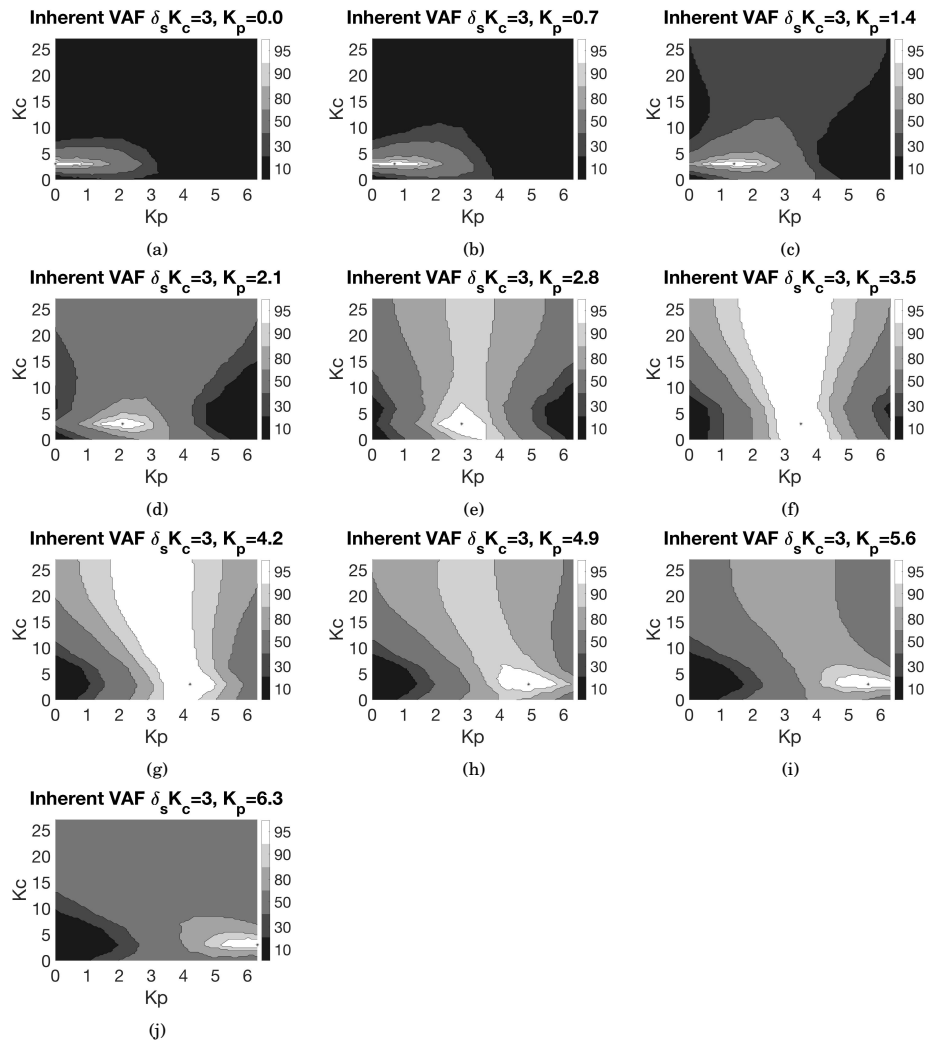


Figure 3: Variance Accounted for Inherent Steering Wheel Angle $K_c=3$, Linear model

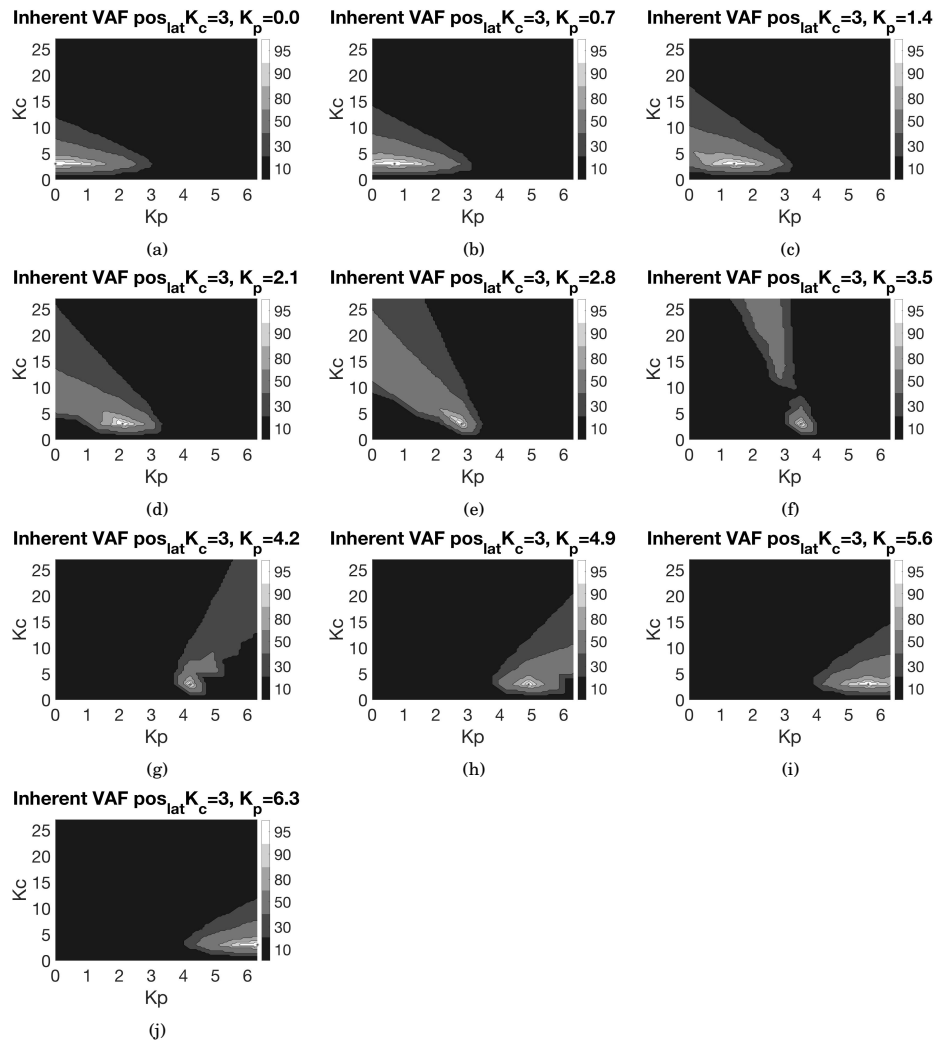


Figure 4: Variance Accounted for Inherent Steering Wheel Angle $K_c=3$, Linear model

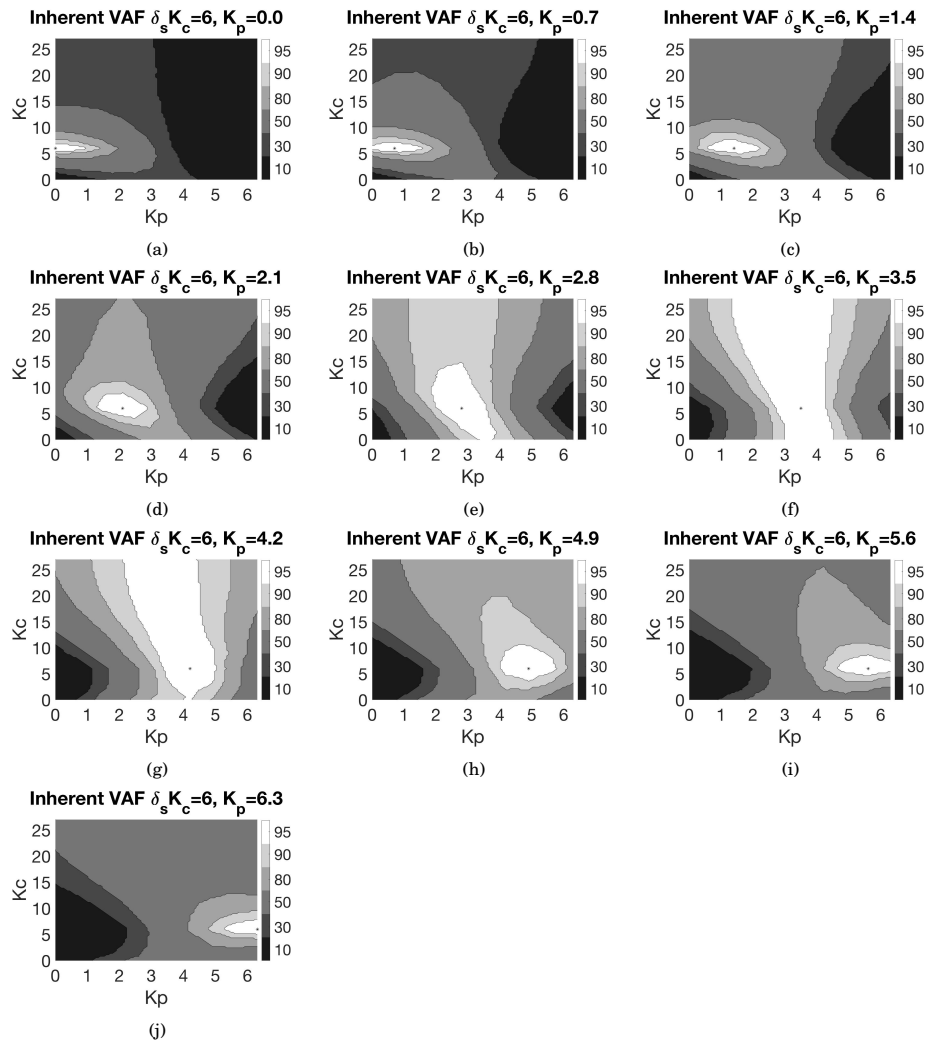


Figure 5: Variance Accounted for Inherent Steering Wheel Angle $K_c=6$, Linear model

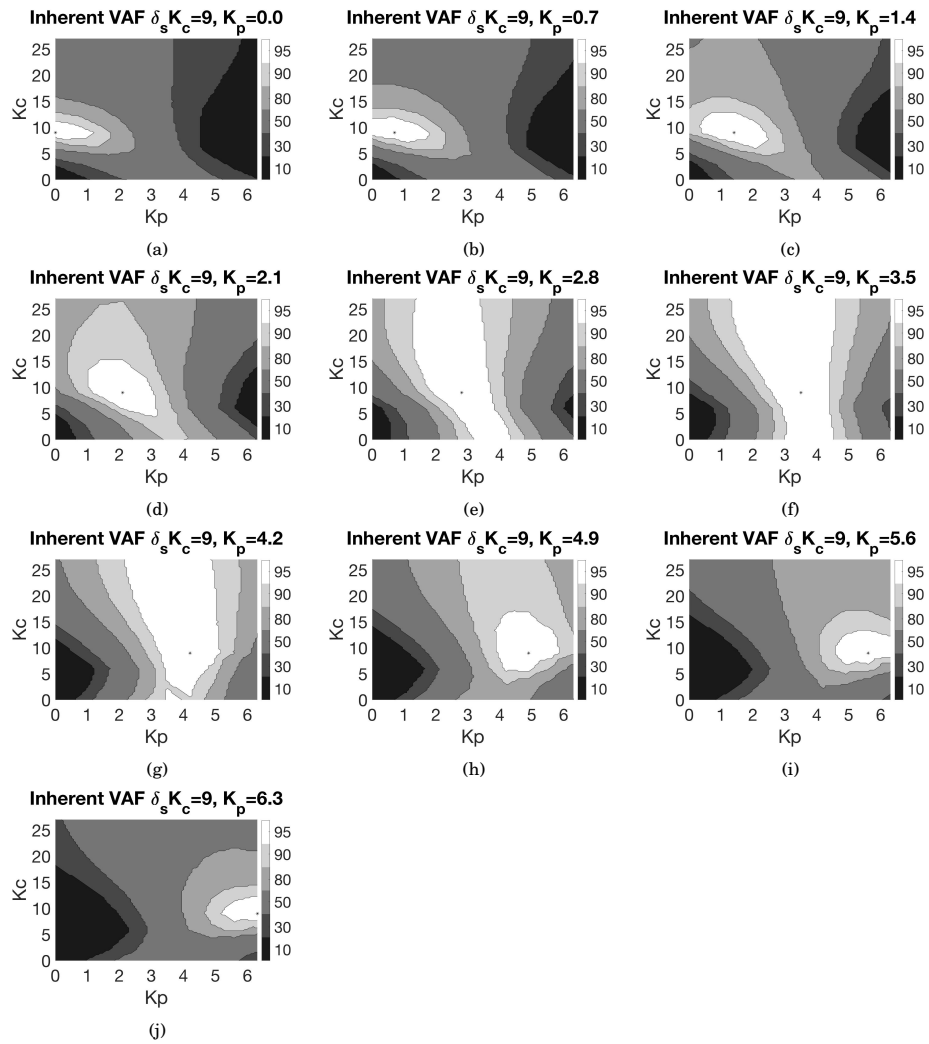


Figure 7: Variance Accounted for Inherent Steering Wheel Angle $K_c=9$, Linear model

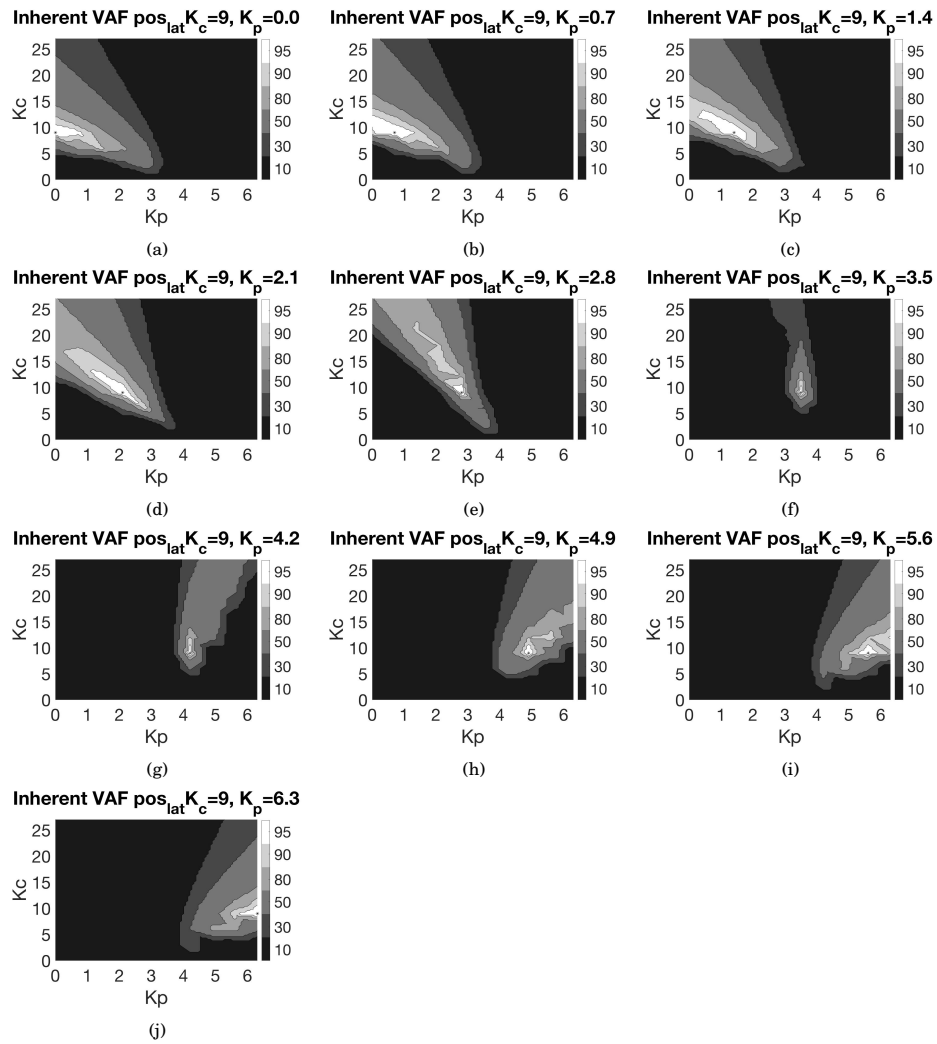


Figure 8: Variance Accounted for Inherent Steering Wheel Angle $K_c=9$, Linear model

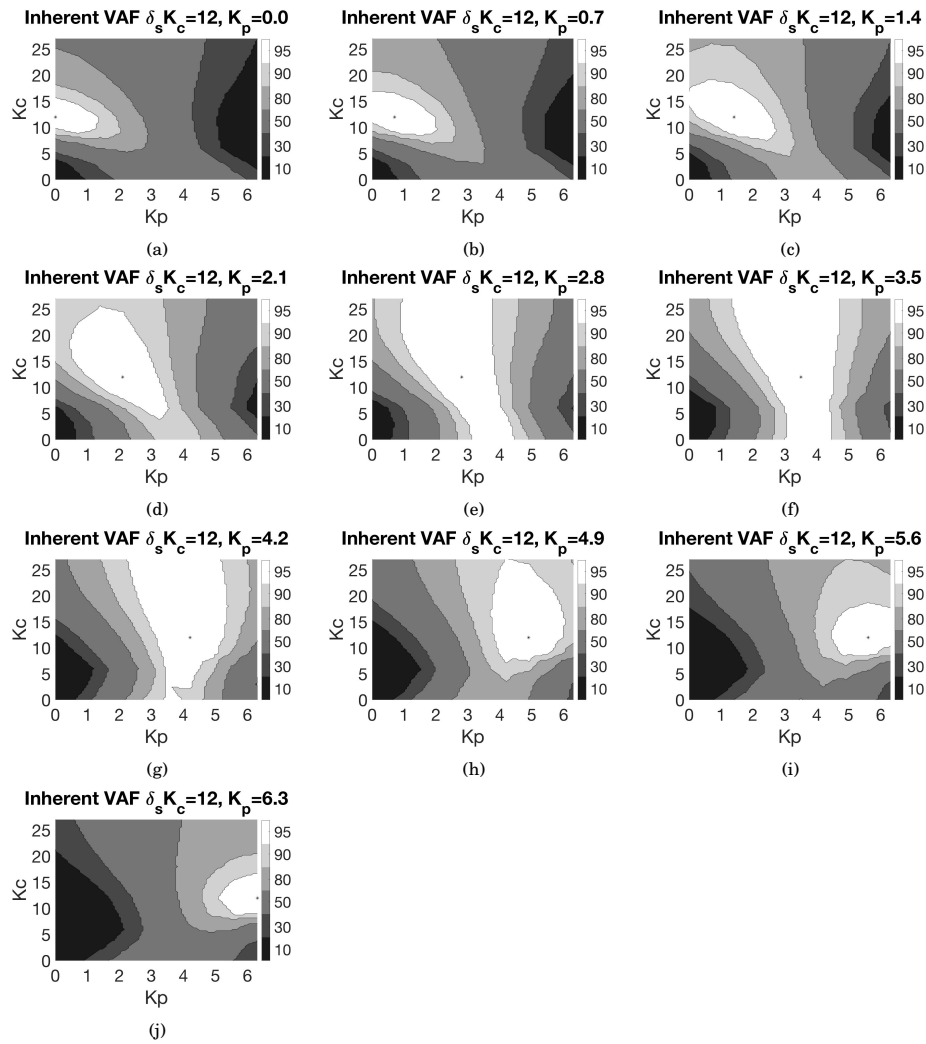


Figure 9: Variance Accounted for Inherent Steering Wheel Angle $K_c=12$, Linear model

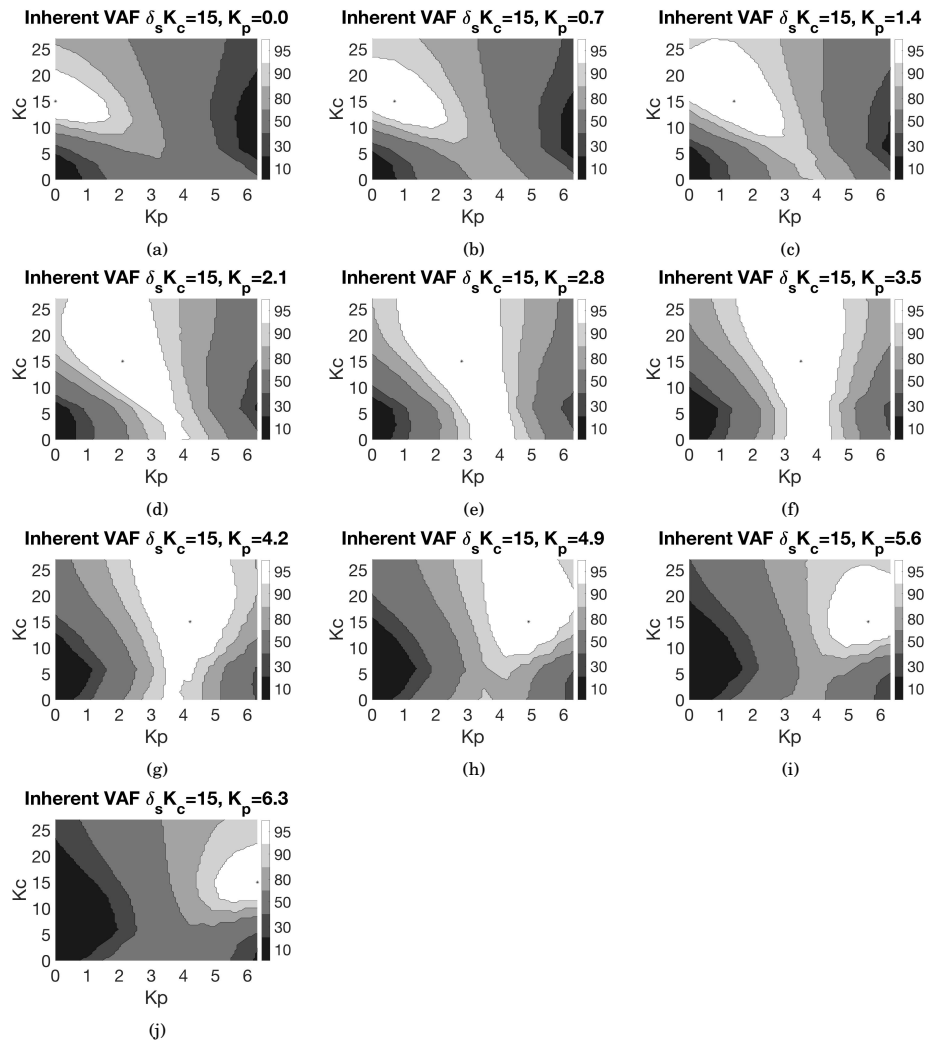


Figure 11: Variance Accounted for Inherent Steering Wheel Angle $K_c=15$, Linear model

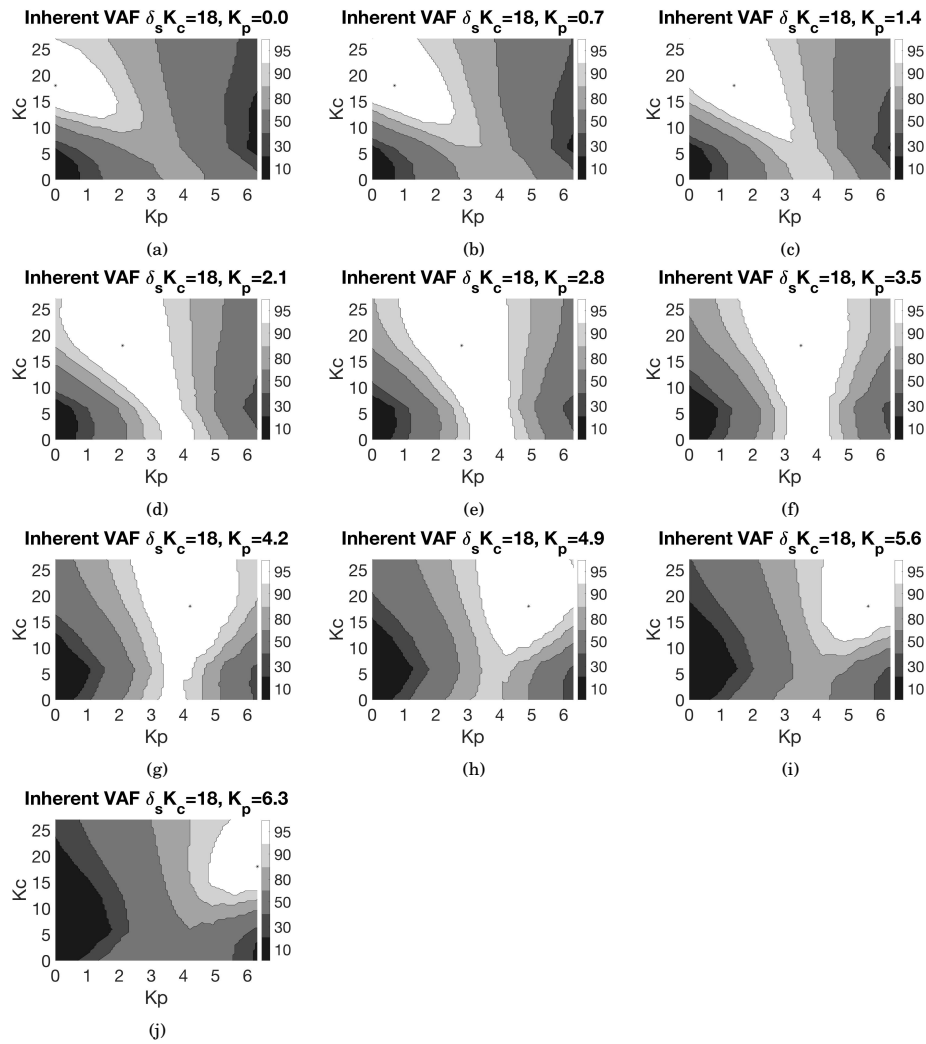


Figure 13: Variance Accounted for Inherent Steering Wheel Angle $K_c=18$, Linear model

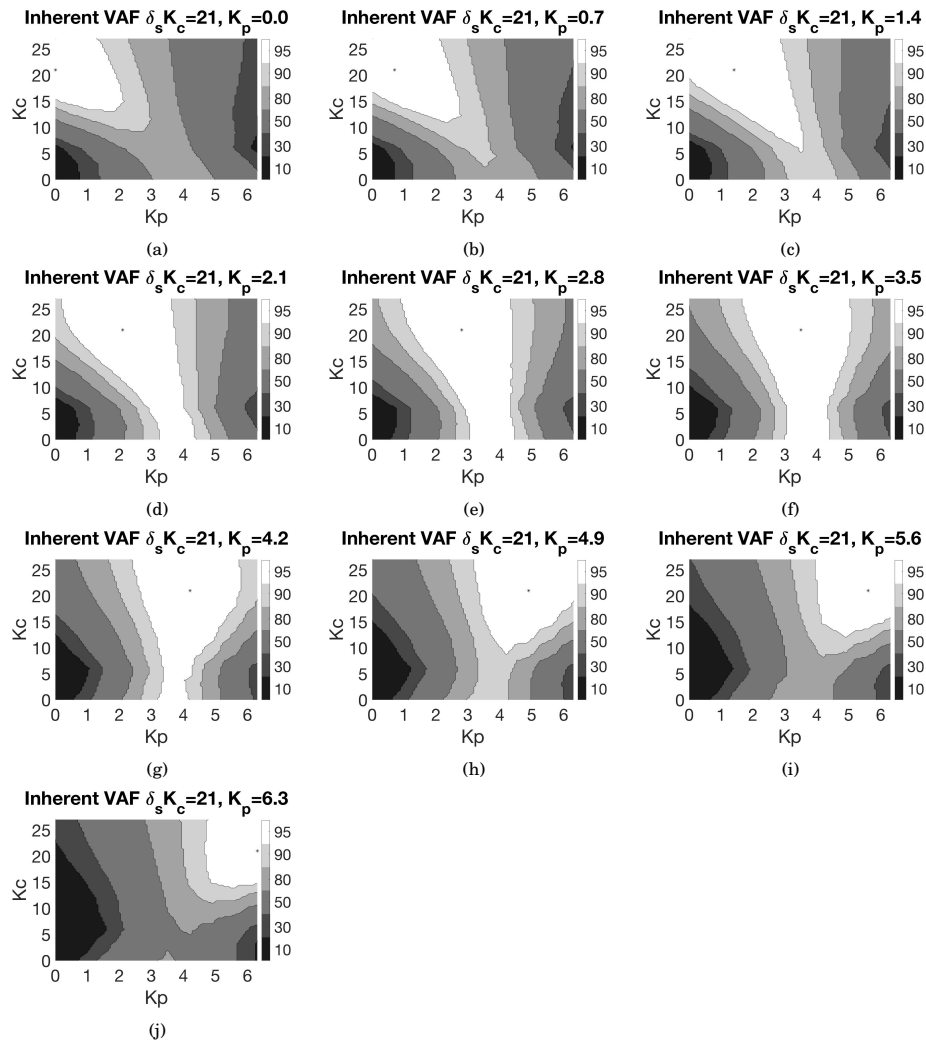


Figure 15: Variance Accounted for Inherent Steering Wheel Angle $K_c=21$, Linear model

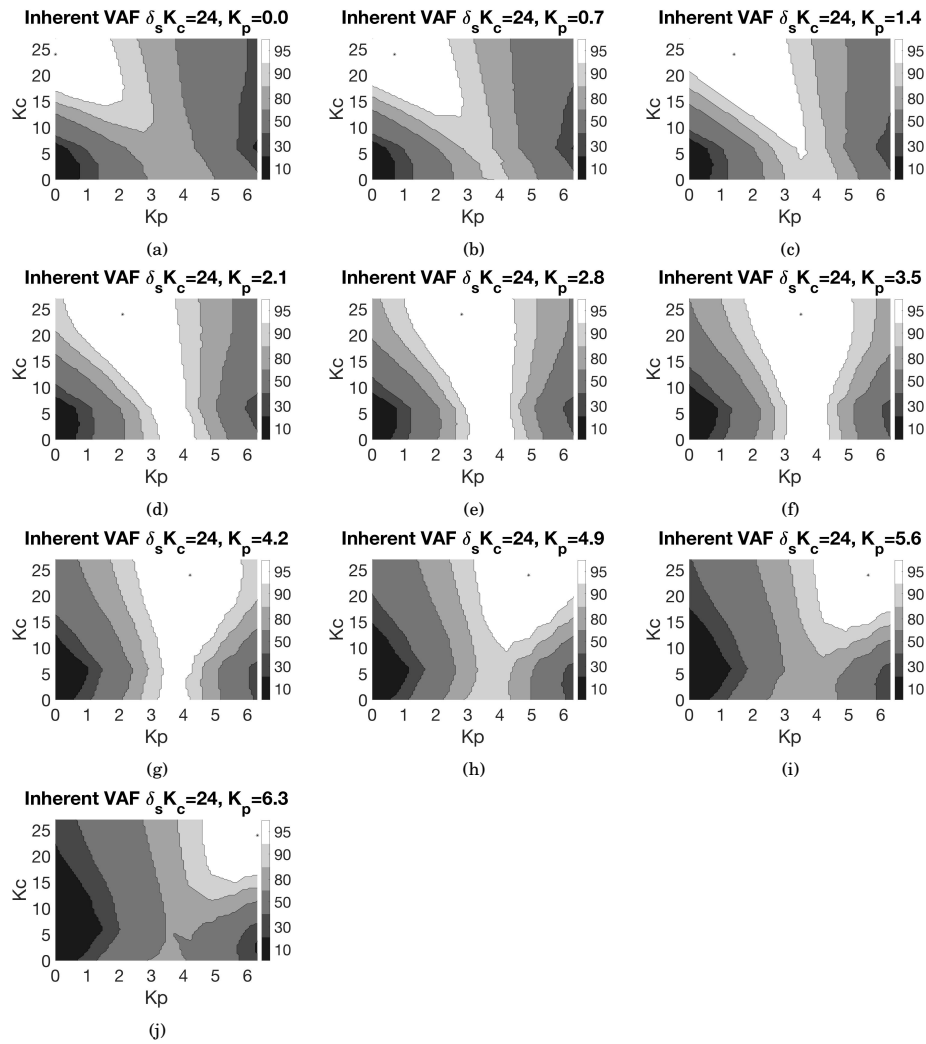


Figure 17: Variance Accounted for Inherent Steering Wheel Angle $K_c=24$, Linear model

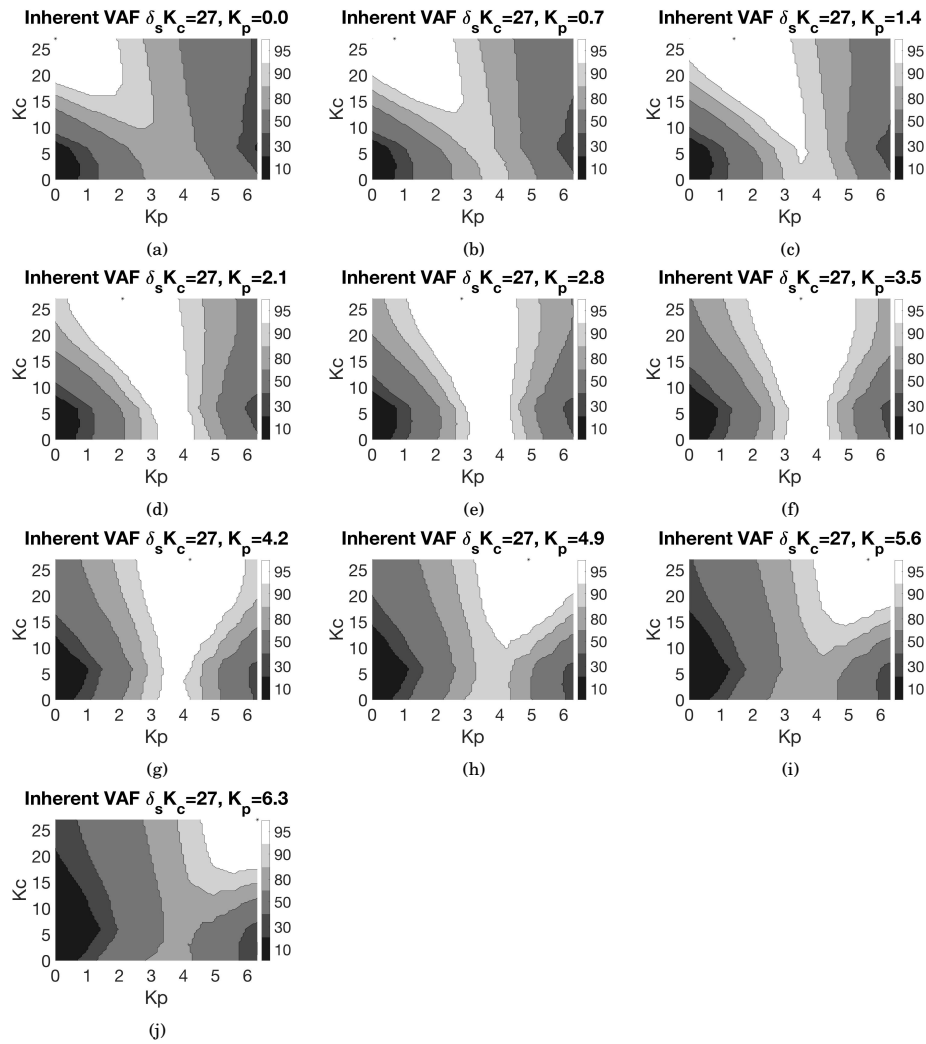


Figure 19: Variance Accounted for Inherent Steering Wheel Angle $K_c=27$, Linear model

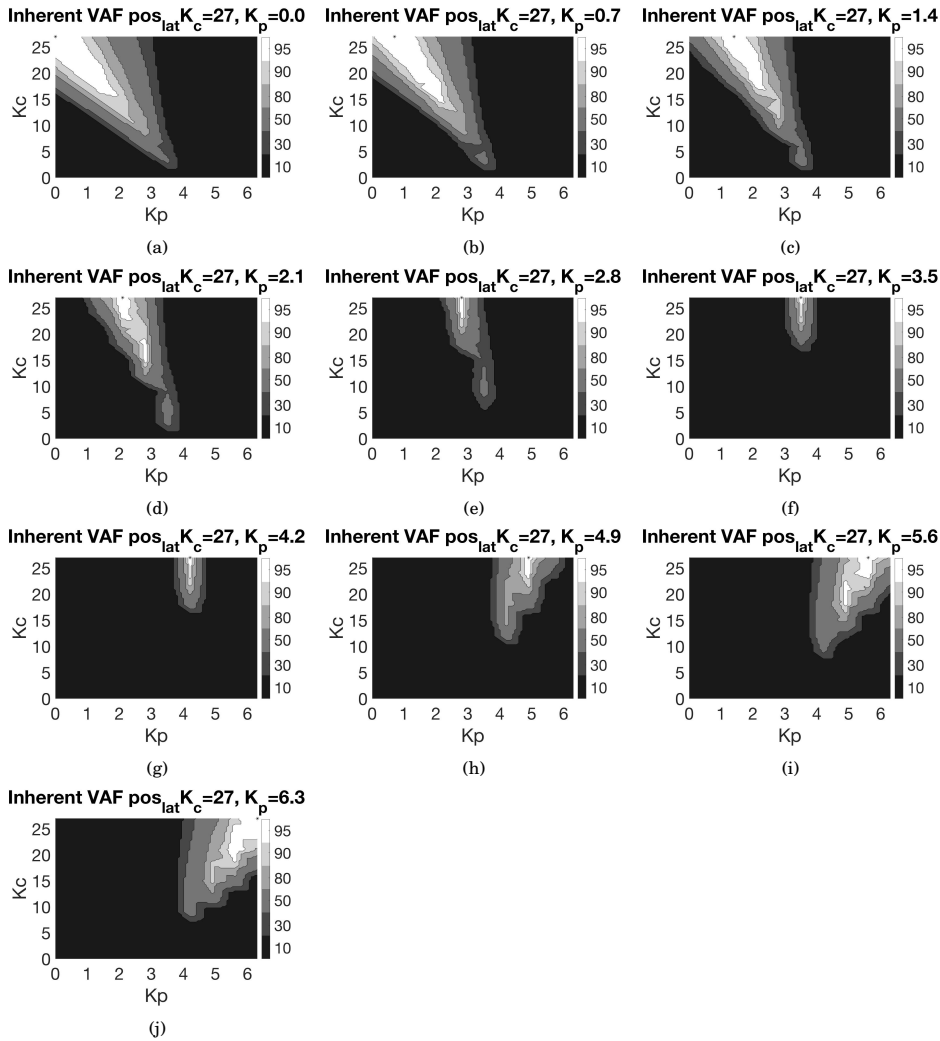


Figure 20: Variance Accounted for Inherent Steering Wheel Angle $K_c=27$, Linear model

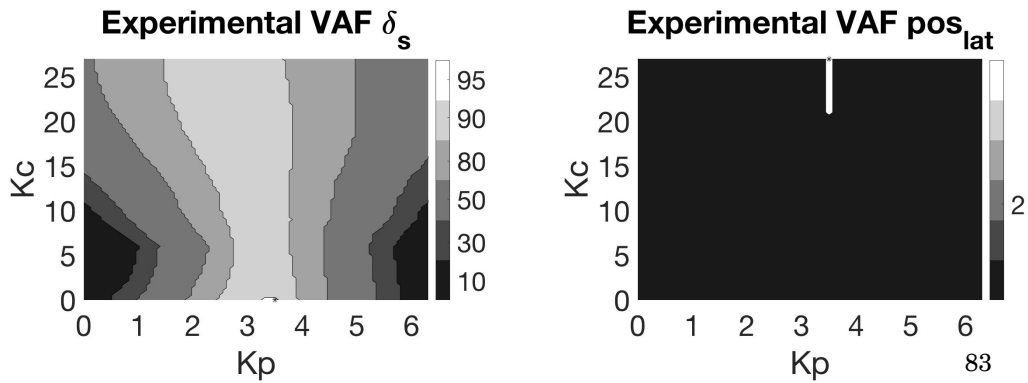


Figure 21: Variance Accounted for Experimental Steering Wheel Angle and Lateral Position, Linear model

Appendix D

Single parameter analysis

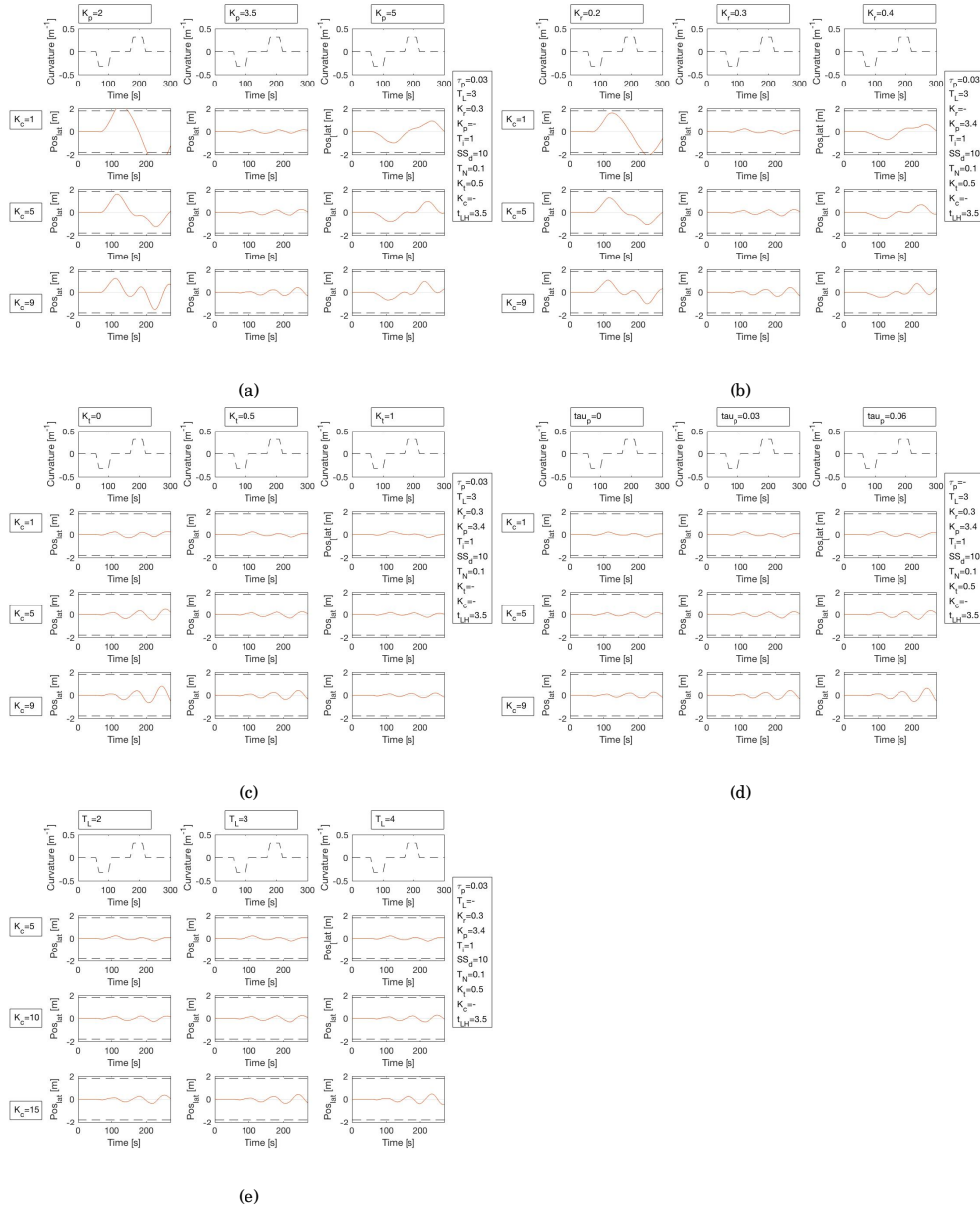


Figure 1: Lateral Position of a simulated car with a differing K_c value and a) K_p , b) K_r , c) K_t , d) τ , e) T_L

During the first phase of this research, a sensitivity analysis was executed where the possible parameter combinations were analyzed on the differentiation in output values they showed, when changing these 2 parameters over a 3 by 3 grid. The outputs which are looked into, are lateral position and steering wheel angle. The parameters values were differentiated in the realistic scope set in the article by Mars(5). Figures 1 to 4 show the output lateral position and figures 5 to 8 the output steering wheel angle. A first interesting combination which was looked into, was the lead and lag time constant combination. They are combined in the compensatory gain block:

$$\frac{T_L s + 1}{T_l + 1} \quad (1)$$

Together they determine the rate and frequencies of near angles to be compensated. Their realistic values seem to fall in a narrow band where the output values don't differ much from each other.

The differentiation's with the K_r and K_t parameters also show significant different output when differentiating over the grid. The neuromuscular loop has been taken out of the model, as explained in the article, so these combinations weren't further looked into.

The combination which shows the biggest differing output, is the combination of the compensation and anticipation gain combination (K_c and K_p). The lateral position output shows both over-turning and curve cutting behaviour, showing a hypothetically wide range of driving behaviour that could be described by differentiating over these two parameters.

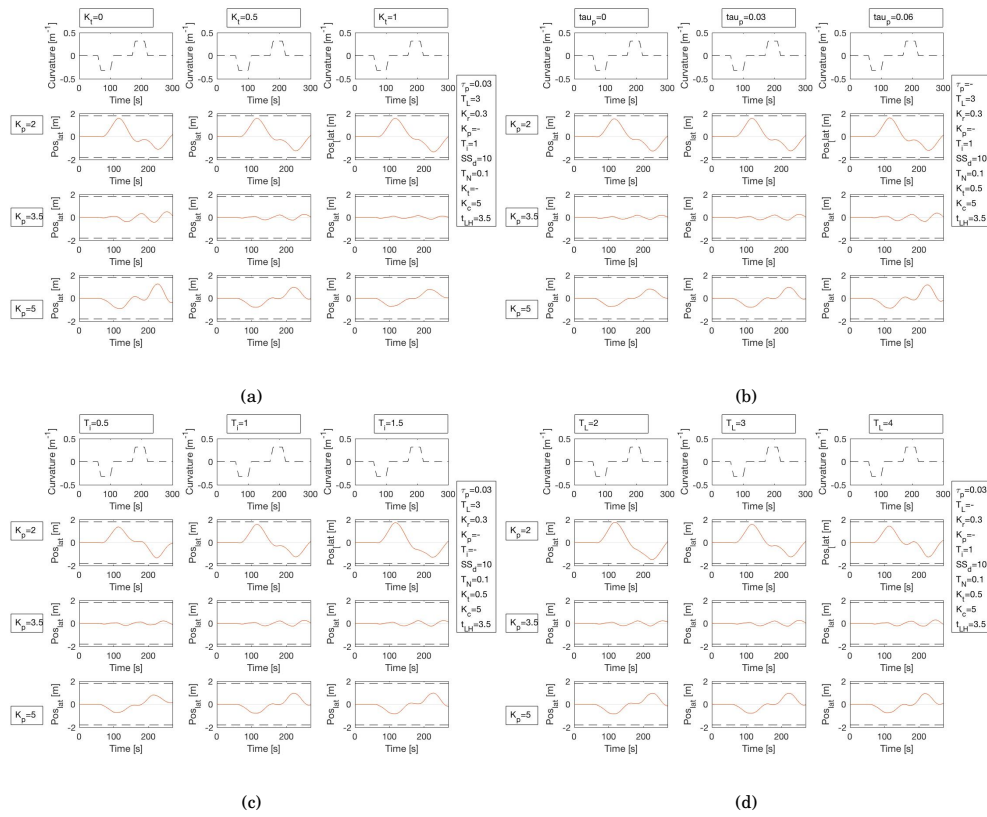


Figure 2: Lateral Position of a simulated car with a differing K_p value and a) K_t , b) τ , c) T_i , d) T_L

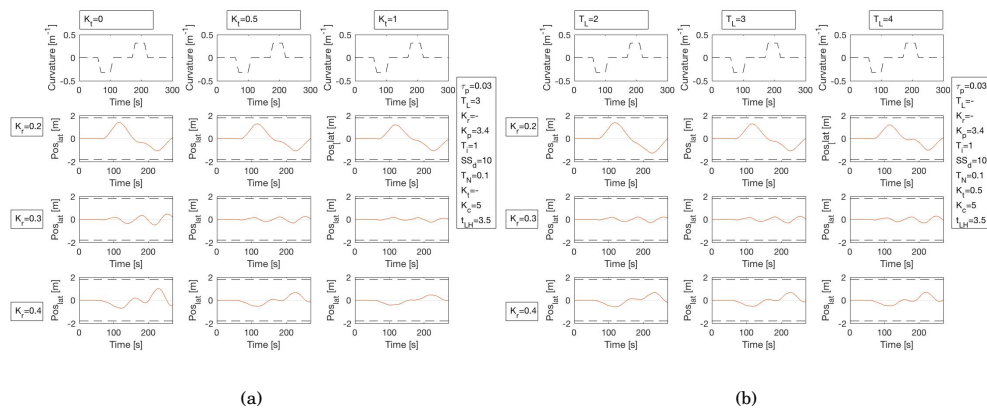


Figure 3: Lateral Position of a simulated car with a differing K_r value and a) K_t , b) T_L

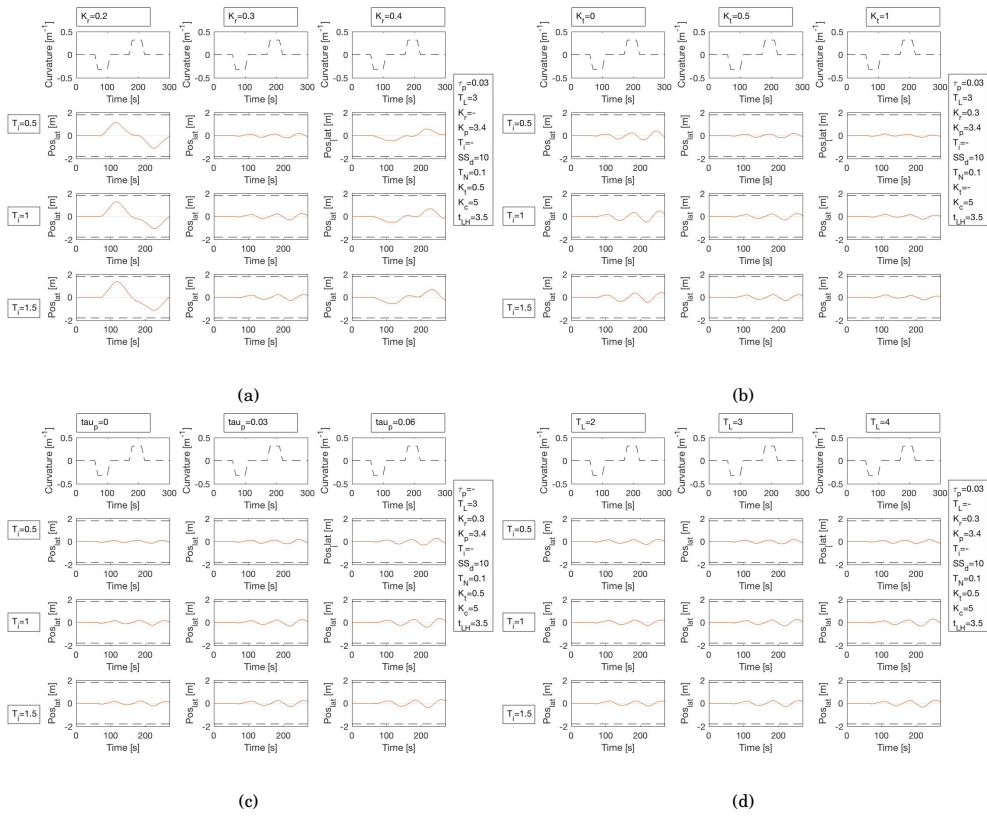


Figure 4: Lateral Position of a simulated car with a differing T_i value and a) K_r , b) K_t , c) τ , d) T_L

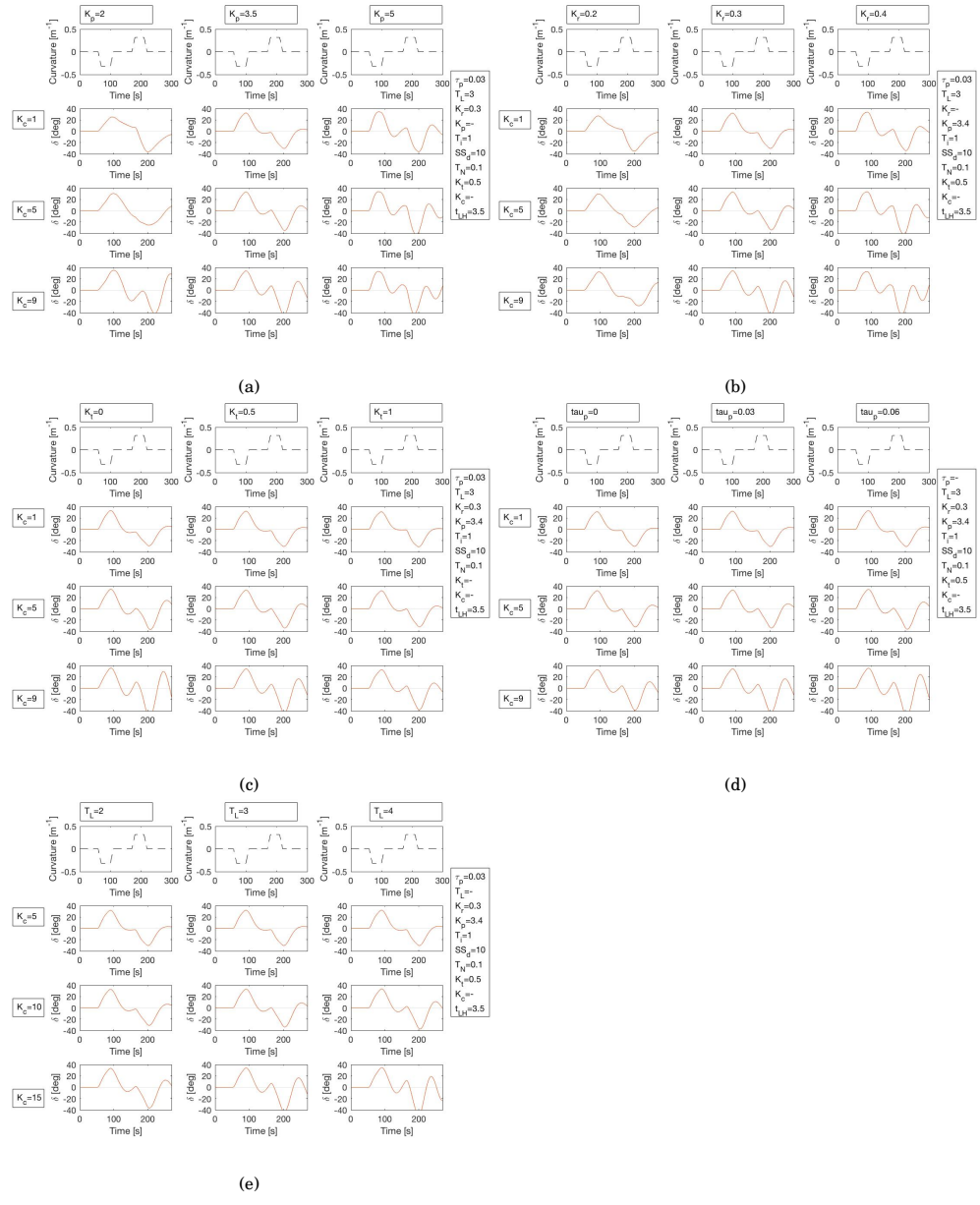


Figure 5: Steering Wheel Angle of a simulated car with a differing K_c value and a) K_p , b) K_r , c) K_t , d) τ , e) T_L

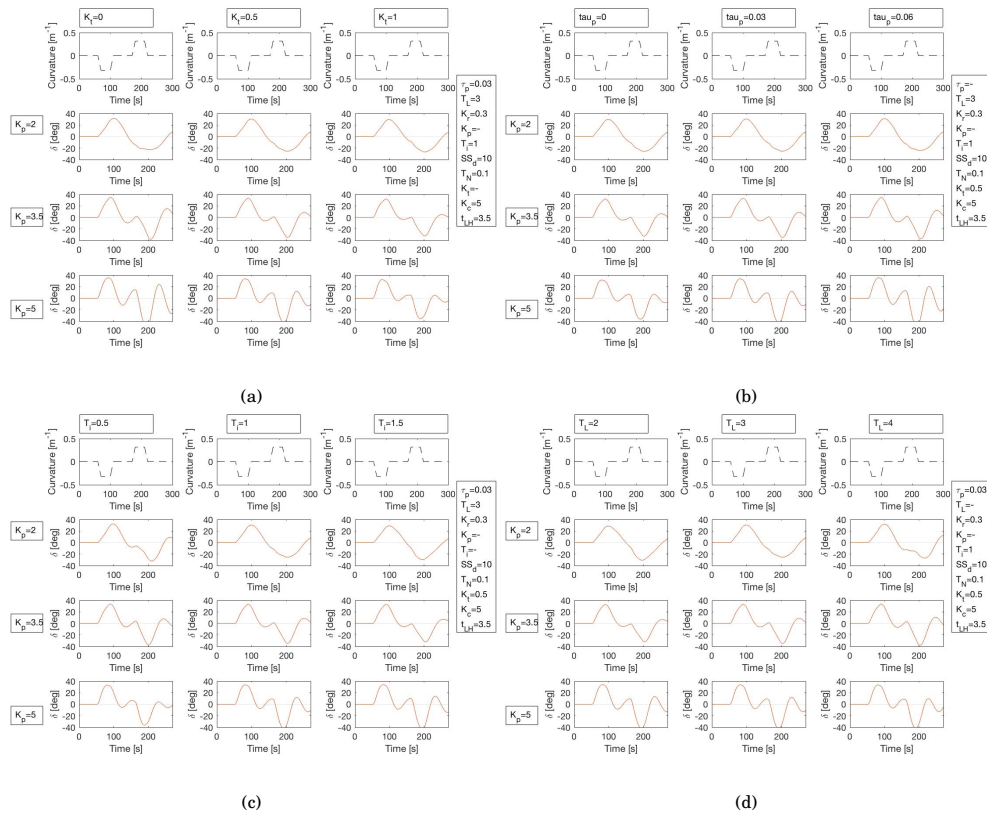


Figure 6: Steering Wheel Angle of a simulated car with a differing K_c value and a) K_p , b) K_r , c) K_t , d) T_L

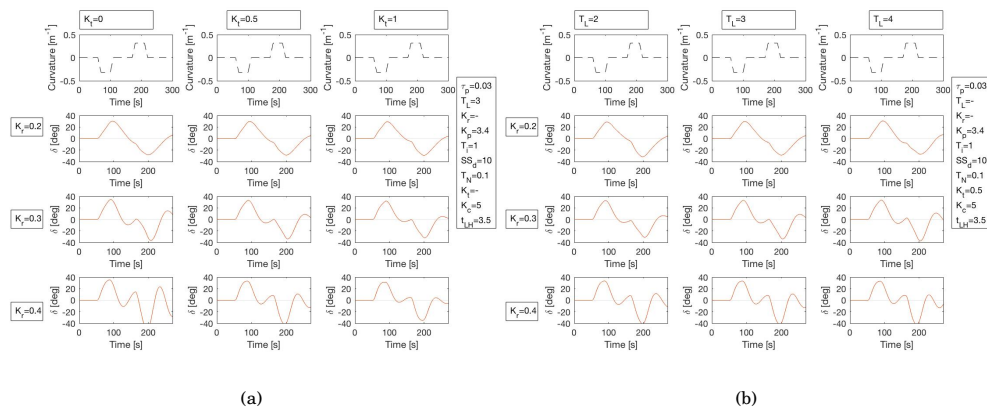


Figure 7: Steering Wheel Angle of a simulated car with a differing K_r value and a) K_t , b) T_L

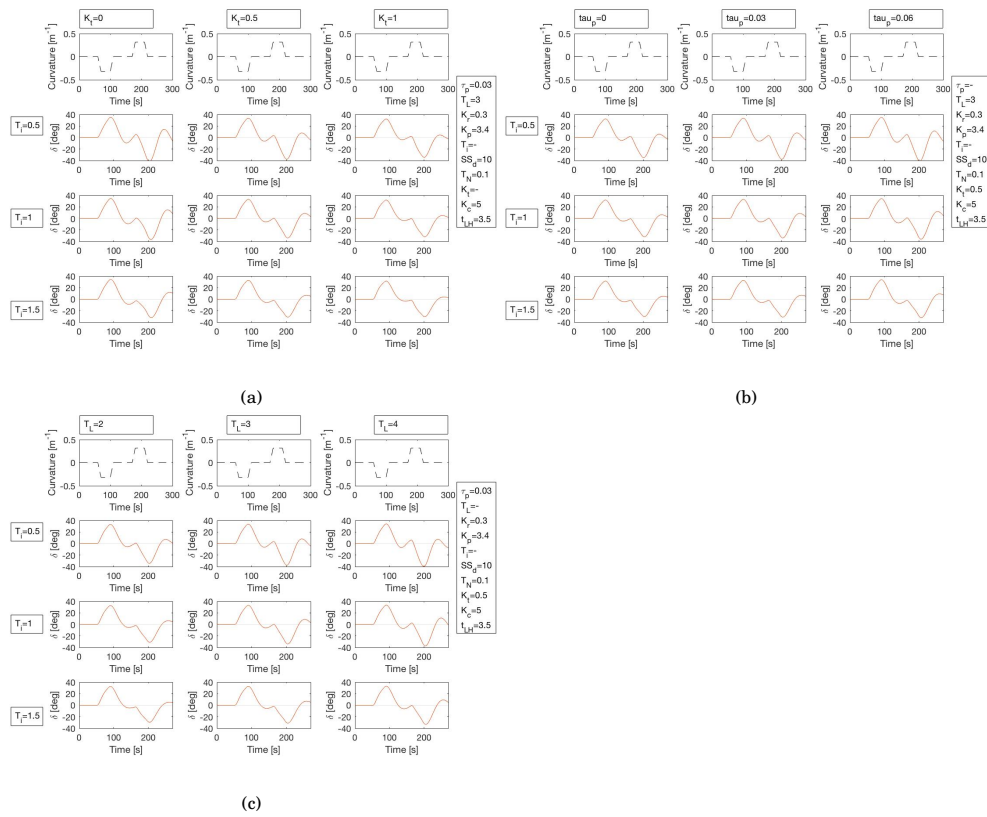


Figure 8: Steering Wheel Angle of a simulated car with a differing T_i value and a) K_t , b) τ , c) T_L